Global and Planetary Change 205 (2021) 103597

Contents lists available at ScienceDirect

Global and Planetary Change

journal homepage: www.elsevier.com/locate/gloplacha

Research paper

How will the progressive global increase of arid areas affect population and land-use in the 21st century?

Jonathan Spinoni *, Paulo Barbosa, Michael Cherlet, Giovanni Forzieri, Niall McCormick, Gustavo Naumann, Jürgen V. Vogt, Alessandro Dosio

European Commission, Joint Research Centre (JRC), Ispra, Italy

ARTICLE INFO

Editor: Jed O Kapan

Keywords:
Arid areas
Climate projections
CORDEX
Land-use
Population
SSPs

ABSTRACT

One of the possible consequences of projected global warming is the progressive enlargement of drylands. This study investigates to what extent population and land-use (forests, pastures, and croplands) are likely to be in areas turning arid in the 21st century. The first part of the study focuses on the climatological enlargement of arid areas at global, macro-regional, and high-resolution (0.44°) scales. To do so we analysed a large ensemble of CORDEX climate simulations, combined three indicators (FAO-UNEP aridity index, Köppen-Geiger climate classification, and Holdridge life zones), and quantified the areas turning from climatologically not arid into climatologically arid (and vice-versa) from recent past (1981–2010) to four projected global warming levels (GWLs) from 1.5°C to 4°C. In the second part, we used population and land-use projections to analyze their exposure to progressive shifts to drier or wetter climate. Both types of projections follow five socio-economic scenarios (SSPs from SSP1 to SSP5). We present results for the viable combinations between SSPs and GWLs. Depending on GWL, the projected drying patterns show regional differences but, overall, the negative consequences of climate change are clear. Already at 1.5°C warming, approximately 2 million km^2 (1.4% of global land) are likely to become arid; at 2°C this area corresponds to 2.6 million km^2 (2.7%), at 3°C to 5.2 million km^2 (3.5%), and at 4°C to 6.8 million km^2 (4.5%), an area that can be ranked the seventh largest country in the World. Such drying is particular strong over South America and southern Europe. In the worst-case scenario (SSP3, regional rivalry, at 4°C), approximately 500 million people will live in areas shifting towards arid climate. Forest areas are likely to be more affected in South America, pastures in Africa, and croplands in the Northern Hemisphere. For land-use, the worst-case scenarios are SSP3 and SSP5 (fossil-fuel based future): at GWL 4°C, about 0.5 million km^2 of forests and 1.2 million km^2 of both pastures and croplands are likely to be in areas shifting to arid climate.

1. Introduction

One of the possible consequences of climate change, projected to accelerate in the next decades (Pachauri et al., 2014), is the progressive enlargement of drylands (Feng and Zhang, 2015). Investigating such enlargement can be challenging, as drylands are complex and evolving systems with no universal definition (Reed et al., 2013). Arid and semi-arid areas are sensitive to climate variability (IPCC, 2018) and highly vulnerable to extreme events such as droughts (Maliva and Missimer, 2012; Greve et al., 2014; Spinoni et al., 2020) and heatwaves (Fu and Feng, 2014), and are prone to fast environmental and land degradation due to limited natural water resources (Dregne, 2002; Glantz, 2019). Such progressive degradation, forced by either natural causes (Geist and Lambin, 2004) or human mismanagement (Mainguet, 2002), can have the potential to challenge the resilience of natural ecosystems, lead to irreversible shifts in their states (D'Odorico et al., 2013; Seidl et al., 2016), and even to irreversible desertification in the worst cases (Reynolds et al., 2007; Veron et al., 2006).

Desertification is a complex phenomenon with manifold causes, its onset is very difficult to anticipate, and its development unpredictable and hard to control (Thomas, 1997; Grainger, 2015; Geist, 2017). Other than by unsustainable land management practices (Imeson, 2012),

* Corresponding author at.: European Commission, Joint Research Centre, Via Enrico Fermi 2749, I-21027 Ispra, (VA), Italy.
E-mail addresses: jonathan.spinoni@ec.europa.eu (J. Spinoni), paulo.barbosa@ec.europa.eu (P. Barbosa), michael.cherlet@ec.europa.eu (M. Cherlet), giovanni.forzieri@ec.europa.eu (G. Forzieri), niall.mccormick@ec.europa.eu (N. McCormick), gustavo.naumann@ec.europa.eu (G. Naumann), juergen.vogt@ec.europa.eu (J.V. Vogt), alessandro.dosio@ec.europa.eu (A. Dosio).

https://doi.org/10.1016/j.gloplacha.2021.103597
Received 22 February 2021; Received in revised form 29 July 2021; Accepted 30 July 2021
Available online 4 August 2021

desertification can be accelerated by climate change towards hotter and drier conditions (Sivakumar, 2007; Verstraete et al., 2009), as observed in the last decades over arid and semi-arid areas in sub-Saharan Africa (Hein and De Ridder, 2006; D'Odorico et al., 2019). Desertification can have devastating impacts on natural resources, from grasslands to shrubs and forests (Von Hardenberg et al., 2001) and a wide variety of land resources (Reich et al., 2001), driving biological processes that can change life cycles (Schlesinger et al., 1990). To combat desertification and limit its impacts, the United Nations' Sustainable Development Goals (UN-SDG) set the specific Goal 15 with the aim of a sustainable use of terrestrial ecosystems (UN General Assembly, 2015).

At global scale, a few studies reported recent enlargement of total arid areas (Feng and Fu, 2013; Spinoni et al., 2015; Cherlet et al., 2018), but opposite greening trends occurred in some areas, especially (but not only) at tropical and sub-tropical latitudes (Fensholt et al., 2012; Zhu et al., 2016; He et al., 2019; Piao et al., 2020). Other studies investigated past drying and wetting trends at different spatial scales over all continents, identifying the desertification hotspots of the last decades: southern Europe (Colantoni et al., 2015; Moral et al., 2016), the Middle-East (Elagib and Abdu, 1997; Kafle and Bruins, 2009), Central Asia (Tabari and Aghajanloo, 2013), China (Wu et al., 2005; Huo et al., 2013), central-eastern Africa (Muhire and Ahmed, 2016), south-western United States (Finkel et al., 2016), southern South America (Adamo and Crews-Meyer, 2006; Nickl et al., 2020), and Australia (Fujioka and Chappell, 2010; Hughes, 2011).

While the overall knowledge of past aridity trends is solid, the understanding of future aridity patterns is still incomplete. Most of the published studies on aridity projections make use – as those on past evolution – of the Food and Agriculture Organization - United Nations Environment Program's Aridity Index (FAO-UNEP AI; Allen et al., 1998), based on the annual ratio between accumulated precipitation and potential evapo-transpiration (PET). However, this method alone can be inappropriate, given that climate models tend to overestimate trends in PET, particularly under extreme climate scenarios (Cook et al., 2014; Milly and Dunne, 2016; Greve et al., 2019). The mentioned studies on aridity projections usually make use of Global Climate Models (GCMs) at medium-low spatial resolution and generally agree on a future expansion of global drylands (Sherwood and Fu, 2014; Roderick et al., 2015; Berg et al., 2016; Fu et al., 2016), also because arid and semi-arid areas are likely to face a steep warming in the 21st century due to land-atmosphere coupling feedback processes (Feng and Fu, 2013; Huang et al., 2016).

Focusing on the climatological aspects of aridity, and in order to make a step forward from current state-of-art of future aridity projections, we constructed – for the first time to our knowledge – global projections of arid areas based on RCMs at high resolution (0.44°). To do that, we used a large ensemble of Regional Climate Models (RCMs) from the datasets of the Coordinated Regional Climate Downscaling Experiment (CORDEX; Giorgi et al., 2009). Following the approach of the third edition of World Atlas of Desertification (Cherlet et al., 2018), we complemented the FAO-UNEP AI with two other indicators, to provide more robust estimations of arid areas: the Köppen-Geiger climate classification (KG; Köppen, 1936; Geiger, 1954), which provides a more refined climate classification than AI (Peel et al., 2007), and the Holdridge Life Zones (HDG; Holdridge and Tosi, 1967), which can be used to incorporate more explicitly ecosystem processes (Lugo et al., 1999).

The main goal of this study therefore consists in estimating to what extent population and selected land-use classes will be exposed to progressive shifts of arid areas at specific Global Warming Levels (GWLs, from 1.5°C to 4°C) and Shared Socioeconomic Pathways (SSPs), which are scenarios of projected socioeconomic global changes for the 21st century and beyond (O'Neill et al., 2014; Riahi et al., 2017; Van Vuuren et al., 2017a; O'Neill et al., 2017).

Scientific studies on human and ecosystems exposure to climatological drying trends towards possible desertification are not new, but they are very rare at global scale. The 3rd edition of WAD reported that population growth and changes in our consumption patterns put unprecedented pressure on global natural resources, analyzing how land and soil degradation, being also linked with deforestation, could lead to displacement of population, reduction in crop yields, and limitations of farmland production (Cherlet et al., 2018).

Other macro-scale studies focused on population in drylands (Safriel, 2009) or in expanding drylands changing with projected warming at global scale (Koutroulis, 2019). Similar studies are focused on the interconnections between drying climate and population at more specific country and regional scales, e.g. for China (Wang et al., 2013), the Mediterranean region (Mendizabal and Puigdefabregas, 2003), or sub-Saharan Africa (Ware, 2019). Studies have also investigated whether drying and desertification processes drive migratory flows (Leighton, 2006; Kniveton et al., 2012). Other works have focused on agricultural lands (Sivakumar et al., 2005; El-Beltagy and Madkour, 2012), forests (Ryan et al., 2008; Zhang et al., 2013), croplands (Powell et al., 2004; Berg et al., 2013), and pastures (Neely et al., 2009; Mu et al., 2013) being part of arid areas subjected to further enlargement (or reduction) driven by climate change (Hansen et al., 2001; Moore and Ghahramani, 2013; Bestelmeyer et al., 2015).

The paper is structured into five parts: after this introduction, Section 2 presents data and indicators used to define arid areas and the methodology to link climatological drying with exposure layers. Section 3 presents maps and tables showing the evolution of arid areas in the 21st century and the projected exposure of population and land-use to drying patterns, with a special focus on the SSP5. Section 4 discusses the drivers of drying and compare our findings with those obtained with land surface indicators. Section 5 summarizes the most relevant findings and hints at further developments.

2. Data and methods

2.1. Climate data

The GCMs model the interactions between climate system components (atmosphere, land surface, ocean, and sea ice) and are used to simulate their evolution for the 21st century and beyond (Semenov and Stratonovitch, 2010). Besides the uncertainties to predict long-term climate processes (Knutti and Sedláček, 2013), one of the major limitations of GCMs is the spatial resolution (Taylor et al., 2012). Such limitation can be overcome by using the RCMs, which include smaller-scale features (Rummukainen, 2010), and consequently lead to improved climate projections (Feser et al., 2011; Kendon et al., 2017; Sørland et al., 2018).

For these reasons, we selected the high-resolution CORDEX simulations for this study. The CORDEX simulations are based on RCMs used to dynamically downscale GCMs (Pielke Sr and Wilby, 2012) from the Coupled Model Intercomparison Project 5 (CMIP5; Taylor et al., 2012), and provide projections with high detail and accurate representation of local-scale physical processes (Giorgi et al., 2009). They have been applied and evaluated over multi-scale (Legasa et al., 2020; Spinoni et al., 2020) and individual domains, showing the added value with respect to using only the GCMs (Martynov et al., 2013; Dell'Aquila et al., 2018; Solman and Blázquez, 2019; Evans et al., 2020). Other publications can be found at: www.cordex.org.

From the CORDEX datasets, we obtained monthly time series of precipitation (P), minimum (TN) and maximum temperature (TX) over 1981–2100. We used all possible GCM-RCM combinations over the fourteen CORDEX regional domains and we selected precipitation and temperature values for two Representative Concentration Pathways (RCP), namely RCP4.5 (Thomson et al., 2011) and RCP8.5 (Riahi et al., 2011). In a future following the moderate emissions scenario (RCP4.5), the highest GWL is 2°C, while higher GWLs (3°C, 4°C, and 5°C over sparse regions; Van Vuuren et al., 2011) can be reached under the assumptions of the more extreme RCP8.5. We excluded other RCPs (e.g., RCP2.6) because only a few simulations – and for a few CORDEX

domains only – were available at the time we gathered data for this study.

Supplementary Table A1 (capital letter A refers to supplementary figures and tables) shows the GCM-RCM combinations used in this study, resulting in an unprecedented number (Fig. A1), ranging from a minimum of 16 (over Antarctica) to a maximum of 145 (over Middle-East). The simulations have been re-gridded over a common 0.44° grid (circa 50 km x 50 km) with no remarkable discontinuities at bordering regions between CORDEX domains (exception being the Urals region, see also Spinoni et al., 2020).

Observed precipitation and temperature data were obtained from the latest version of the Deutscher Wetterdienst's Global Precipitation Climatology Centre (GPCC; Schneider et al., 2018) and the University of East Anglia's Climate Research Unit (CRU; Harris et al., 2020). These datasets have been used to derive arid areas and the climatological shift to arid climate over past decades in the 3rd edition of WAD (Cherlet et al., 2018) and therefore represent a reliable source to validate results obtained with CORDEX simulations over 1981–2010.

2.2. Indicators to delineate arid areas

As anticipated in Section 1, in this study arid areas are defined by means of three indicators. The reason behind this choice is to complement an indicator specifically designed to focus on drylands (AI) with two additional indicators including climate-based (KG) and vegetation-based (HDG) definitions of aridity, though they all use meteorological data as input. A similar multi-indicator approach was applied by Spinoni et al. (2015) to quantify global arid areas for the period 1951–2010.

AI is based on the annual ratio between total precipitation (P) and PET and is characterized by four main classes (Arid, Normal, Humid, and Cold) and eight sub-classes (Cherlet et al., 2018). In this study, we focus on the main class Arid with its four sub-classes (Desert, Hyper-arid, Arid, and Semi-arid), that correspond to annual P/PET $\leq$0.5 on average. For AI (and HDG), PET was calculated with the Hargreaves-Samani's equation (Hargreaves and Samani, 1985).

The second indicator, KG, requires 30-year averaged monthly and seasonal precipitation and temperatures to form a set of fourteen conditions and divides climate into to five main classes (Tropical, Arid, Temperate, Boreal, and Polar) and thirty sub-classes or more, depending on peculiar choices on very cold climates (Belda et al., 2014). Here, we selected the main class Arid, with its four subclasses (Cold and Hot Desert, Cold and Hot Steppe), that correspond to an annual total precipitation (in mm) smaller than twenty times the sum of annual average temperature plus a constant value of 0, 14 or 28, which depends on the seasonal distribution of precipitation (Kottek et al., 2006).

The KG classification is arguably the most widespread climate classification applied at global scale for past (Kottek et al., 2006; Peel et al., 2007) and future climate classification (Rubel and Kottek, 2010; Beck et al., 2018). It has also been used at regional scales over most regions of the World (Crosbie et al., 2012; Alvares et al., 2013; Chan et al., 2016; Engelbrecht and Engelbrecht, 2016; Rubel et al., 2017), and to define climate zones linked with biomes and ecosystems (Rohli et al., 2015).

HDG is based on a pyramidal classification scheme from 30-year averaged quantities: precipitation, the ratio PET/P, and bio-temperature, which is based on monthly temperature and thresholds (0°C and 30°C) assumed to represent the lower and upper limits of plant growth (Holdridge and Tosi, 1967). However, we set the upper threshold to 35°C because, in view of progressive global warming, plants may adapt, especially in tropical zones (Holdridge and Grenke, 1971; Jump and Penuelas, 2005; Colwell et al., 2008), whereas the lower threshold is unchanged as for plants it is more difficult to adapt to cold climates (Körner and Larcher, 1988). The number of classes in the HDG system ranges between thirty-one and thirty-six, due to a variable number of subdivisions for cold climate (Szelepcsényi et al., 2014). In this study, to delineate arid areas using HDG, we selected the sub-classes desert, desert scrub, thorn woodland, thorn steppe, and very dry forest (see the naming scheme in Lugo et al. (1999). Such classes are characterized by annual PET to precipitation ratio larger than 2, annual precipitation below 1000 mm, and bio-temperature higher than 3°C.

The HDG method is commonly applied to classify zones according to mixed vegetation and climate features, as in Lugo et al. (1999), Chen et al. (2003), Ze-meng and Tian-xiang (2005), Szelepcsényi et al. (2018), Tatli and Dalfes (2016), Derguy et al. (2019).

Since the choice of the underlying climate classification indicator can play a prominent role in the delineation of climatologically arid areas, we opted for the combined use of the three indicators. Firstly, for each point of the common global grid we separately computed the three indicators, using each simulation available for the corresponding point, keeping in mind that a variable number of GCM-RCM simulations (Table A1) is available for each grid point (Fig. A1). Secondly, and yet separately for the three indicators, we assigned to the grid point the predominant climate class, which is the class detected by the largest number of simulations over that particular point. Thirdly, we considered the point to be "arid" if it falls in the arid class for at least two of the mentioned indicators and "not arid" if it falls in the arid class for one (or none) indicator only.

We specifically focus on shifts of climatologically arid areas, i.e. on areas that are climatologically arid in recent past (RP, 1981–2010) and are projected to shift to a climatologically not-arid class in the future (at a specific GWL) and, oppositely, on areas that are climatologically arid in 1981–2010 and are projected to shift to climatologically not-arid at a specific GWL. From now on, when we refer to arid areas we omit *climatologically*.

To obtain the changes in arid areas between RP and GWLs (from 1.5°C to 4°C), we followed the approach described in Dosio and Fischer (2018). Let us choose GWL1.5°C as example, which represents a global average temperature increase of 1.5°C from pre-industrial period. Between 1881–1910 (representing the pre-industrial era in this study; Hawkins et al., 2017) and 1981–2010, the average global temperature increased by 0.96°C, according to the NASA Goddard's Global Surface Temperature Analysis dataset (GISTEMPv4; Hansen et al., 2010). Thus, to reach GWL1.5°C, we had to find the 30-year period (in the future) with additional 0.54°C difference from 1981–2010, using the ensemble median of the combinations of GCMs and RCPs. Such 30-year interval therefore refers to GWL1.5°C and an identical procedure, respectively focusing at additional 1.04°C, 2.04°C, and 3.04°C from 1981–2010, is applied to obtain the 30-year intervals referring to GWL2°C, GWL3°C, and GWL4°C.

2.3. Population and land-use data and exposure to climatological shifts

Population projections are derived from the NASA-SEDAC dataset, which includes data for the period 2000–2100, selecting for this study total population, without distinguishing between rural and urban population. They are provided at high spatial resolution (0.125°), they are qualitatively and quantitatively consistent with the SSPs (Jones and O'Neill, 2020), and have been recently applied to other studies dealing with population exposure to future climate change (Batibeniz et al., 2020). We assumed that the base year (2000) represents 1981–2010, and, from the NASA-SEDAC dataset, we selected data five SSPs (SSP1 to SSP5; O'Neill et al., 2017).

Each SSP describes a socioeconomic development based on a special narrative, leading to different population and land-use evolution in the 21st century. The SSP1 ("green growth"; Van Vuuren et al., 2017b), describes a development with sustainable consumption of resources and energy. The SSP2 ("middle of the road"; Fricko et al., 2017) foresees socioeconomic future in line with historical trends, global moderate population growth (but larger than SSP1) with a leveling in the second half of the century, and slow decline of resources. The SSP3 ("regional rivalry", Fujimori et al., 2017) is based on policies oriented to national laws on food security, energy, and resources, with a high environmental risks and high population increase in industrialized and developing

countries. The SSP4 ("deepening inequality"; Calvin et al., 2017) combines increasing inequalities within countries with large investments in both carbon-intensive and low-carbon energy sources, with population growth similar to SSP2. The SSP5 ("fossil-fueled development"; Kriegler et al., 2017) represents the least sustainable scenario, together with the SSP3, with fast growth of the global economy, strong globalization, uncontrolled exploitation of fossil-fuel resources, and limited attention to environmental impacts.

In this study, land-use projections are derived from the Land-Use Harmonization[2] (LUH2) datasets. The LUH2 project produces a harmonized ensemble of land-use scenarios connecting the historical reconstructions and the future projections of land-use (Hurtt et al., 2020) and its data have been recently applied to climate change studies (Krause et al., 2019; Yu et al., 2019). To ensure consistency with population projections, we selected LUH2 annual data for SSPs from SSP1 to SSP5, from 1981 to 2100, and at 0.25° resolution data

We focused on three main classes: croplands, pastures, and forested areas. The cropland fraction of each grid cell is the sum of five different crop functional types: C_3 plants (annuals, perennials), C_4 plants (annuals, perennials), and C_3 nitrogen fixers plants; see Pearcy and Ehleringer (1984) for details on C_3 and C_4 plants. Dealing with pastures, only managed pastures are included in the analyses. Forested areas result from the sum of forested primary (never impacted by human activities) and secondary (recovering by human disturbance) vegetation. More details on the LUH2 classes in Hurtt et al. (2020) and at: https://luh.umd.edu/.

LUH2 is a land-use product and focuses at the human use of the land, so the differentiation between forested and non-forested vegetation acts like a first-order land cover classification (Ma et al., 2020), but it is not free from uncertainties. However, known uncertainties in land cover projections (Alexander et al., 2017) are generally as large as those for land-use (Dendoncker et al., 2008; Prestele et al., 2016), in particular for forests (Bradley et al., 2017).

We calculated the number of people and the percentage of land area (for the three land-use classes) exposed to a significant decrease in average annual total precipitation between 1981–2010 and 30-year periods corresponding to the four GWLs. In this study, a change of a variable (or class) between two 30-year periods is defined as significant if at least two-thirds climate simulations used for that grid point project concordant sign for such change. Then, we computed the number of people and the land-use surface within arid areas in 1981–2010 and at the four GWLs. Finally, we derived the number of people and the land-use extent in areas that are arid at selected GWLs and were not arid in 1981–2010. We performed the analyses at different aggregation scales: global, continental, macro-regional (Fig. A2), and grid-point (0.44°).

3. Results

3.1. Hotspot areas facing future climatological drying trend

Before investigating the future extent of arid areas, we performed a double validation exercise. Firstly, we compared arid areas over 1981–2010, obtained with observational datasets (GPCC and CRU) and climate simulations (CORDEX ensemble): all indicators show no disagreement between models and observations except over South America (especially Argentina), AI and HDG also over the central United States, but no other clear discrepancies are found (Fig. A3). Secondly, we analyzed if CORDEX results agree on the delineation of arid areas according to all indicators, and we found very limited inter-model differences, visible in the central United States, the Sahel, central India, and Mongolia, and especially using AI (Fig. A3).

Analysis of single indicators shows comparable results in absolute values both at global and continental scales (Fig. A4–A5–A6), with a progressive increase of arid areas with increasing GWLs. The only exception is North America where – despite all subregions showing a projected large and significant temperature increase (Table A2) – the projected precipitation increase causes the extent of arid areas to decrease according to AI (Table A3). Though at regional scale the differences can be substantial, the extent of arid areas calculated with KG is generally smaller, in both Hemispheres, than that with AI or HDG.

When the three indicators are combined (Table 1 and Fig. 1), we found that arid areas are projected to increase at global scale and replace 1.1% of other climate zones at GWL 1.5°C (increase of 1.6 million km^2), 1.4% at GWL 2°C (2.1 million km^2), 3% at GWL 3°C (4.6 million km^2), and 3.8% at GWL 4°C (5.6 million km^2). This is due to a global consistent increase of areas shifting from not arid in 1981–2010 to arid in the future (6.78 million km^2, the 4.6%, at GWL 4°C), with the largest values in South America (2.14 million km^2 at 4°C) and Asia (1.83 million km^2 at 4°C). Conversely, the global extent of areas shifting from arid in 1981–2010 to not arid in the future is much smaller (1.15 million km^2, the 0.8%, at GWL 4°C), with largest values for Africa (0.45 million km^2 at 4°C) and Asia (0.38 million km^2 at 4°C).

Fig. 1 shows that most of arid and semi-arid zones in the World will enlarge with increasing GWLs and the shift from not arid to arid is larger, in absolute values, over the Northern Hemisphere, though in percentage values it is larger over the Southern Hemisphere (excluding at GWL 1.5°C). The areas shifting towards arid climate are: the Mojave and Sonoran deserts (North America), north-eastern Brazil, northern Bolivia, the Atacama desert (Chile), Patagonian steppe (Argentina), the Mediterranean region, the Namib and Kalahari deserts (southern Africa), the steppe in Russia, Kazakhstan, and Mongolia, the Thar desert (India), south-eastern China, and semi-arid central Australia both westwards and eastwards. Oppositely, a retreat of arid areas is projected for the Mid-West U.S. already at GWL 2°C, southern Tchad, and Hebei and Beijing provinces (China) at GWL 3°C, and central-southern India at GWL 4°C. Mixed patterns are projected for the central U.S. and the Sahel, where inter-model variability is the highest (see, Dosio et al., 2020).

Table 1 shows that the progressive enlargement of arid areas is likely to occur in all continents, but in few macro-regions the fraction of arid areas likely to retreat is larger than the fraction experiencing the opposite process (Fig. 2): this occurs from 1.5°C warming in central-eastern Africa, from 2°C warming in central Africa, and from 4°C warming in western Africa and southern Asia. In absolute values (Table A4), the hotspots with the largest areas shifting towards arid climate are Amazonia, the Mediterranean region, north-western and eastern Asia, all with more than 0.5 million km^2 at GWL 4°C. Other macro-regions showing large values (>0.25 million km^2 at GWL 3°C) are central North America, south-western and south-eastern South America, north-eastern Brazil, and south-western and south-eastern Africa.

3.2. Population exposed to a drying climate and enlargement of arid areas

According to our analyses, temperature is projected to increase in every macro-region but the sign of future change in mean precipitation is uncertain is some regions (see also Dosio et al., 2019; Dosio et al., 2020), though precipitation is overall projected to slightly increase at global scale (Table A2). At global scale, the SSP3 represents the worst-case scenario (excluding North America and Oceania) for the population exposed to significant precipitation decrease, with approximately 1.7 billion people at GWL 4°C (Fig. A7). This occurs also because the SSP3 projects the largest population increase in the 21st century. In percentage (Table A5), population exposed to significant drying is about 7% at GWL 1.5°C and GWL 2°C (with any SSP) and above 10% at GWLs 3°C and 4°C, with maximum exposure at GWL 4°C with SSP3 (13.9%). Europe is the continent showing the largest exposure (>35% already at GWL 2°C with any SSP).

Temperature increase, mixed precipitation tendencies, and global population increase, lead to overall increase of population in arid areas with any SSP-GWL combination. Globally, the population living in arid areas is projected to increase from approximately 1.4 billion in 1981–2010 to values above 2.5 billion (SSP2, SSP3, and SSP4 from GWL

Table 1
Left: Areas (10^6 km^2 and %) climatologically arid in 1981–2010 (RP) and at GWLs. Centre: areas likely to turn from not arid (RP) to arid at GWLs. Right: areas likely to shift from arid (RP) to not arid at GWLs. See Fig. A2 for continents.

		Arid					Not Arid to Arid				Arid to not Arid			
Area	Region	RP	1.5°	2°	3°	4°	1.5°	2°	3°	4°	1.5°	2°	3°	4°
	N_AM	2.80	3.05	2.93	3.20	3.22	0.29	0.27	0.55	0.52	0.05	0.14	0.15	0.11
	C_AM	0.82	0.91	0.92	1.08	1.02	0.11	0.12	0.27	0.23	0.01	0.02	0.00	0.03
	S_AM	3.64	3.90	4.00	4.94	5.62	0.40	0.52	1.40	2.14	0.14	0.16	0.10	0.16
	EUR	2.59	2.77	2.87	3.22	3.40	0.20	0.30	0.63	0.81	0.02	0.02	0.00	0.00
	AFR	18.28	18.45	18.50	18.78	18.75	0.28	0.38	0.77	0.92	0.12	0.17	0.27	0.45
	ASIA	14.56	15.07	15.31	15.70	16.00	0.56	0.84	1.26	1.83	0.05	0.09	0.12	0.38
	OCE	6.21	6.40	6.47	6.55	6.52	0.19	0.26	0.34	0.32	0.00	0.01	0.00	0.01
10^6 km^2	**WORLD**	**48.91**	**50.55**	**51.01**	**53.46**	**54.54**	**2.02**	**2.70**	**5.21**	**6.78**	**0.39**	**0.59**	**0.66**	**1.15**
	N_AM	12.69	13.78	13.28	14.48	14.56	1.31	1.23	2.47	2.37	0.22	0.64	0.68	0.50
	C_AM	27.80	30.96	31.36	36.64	34.69	3.63	4.11	8.99	7.91	0.47	0.55	0.16	1.03
	S_AM	19.70	21.09	21.68	26.72	30.42	2.15	2.84	7.58	11.58	0.75	0.86	0.57	0.85
	EUR	25.21	26.96	27.95	31.33	33.07	1.90	2.89	6.12	7.86	0.15	0.15	0.00	0.00
	AFR	61.40	61.96	62.11	63.07	62.97	0.95	1.28	2.59	3.10	0.39	0.56	0.92	1.52
	ASIA	30.75	31.83	32.34	33.15	33.80	1.19	1.77	2.67	3.86	0.11	0.18	0.26	0.81
	OCE	70.00	72.10	72.87	73.74	73.49	2.13	2.95	3.79	3.62	0.02	0.08	0.05	0.13
%	**WORLD**	**32.96**	**34.06**	**34.37**	**36.02**	**36.75**	**1.36**	**1.82**	**3.51**	**4.57**	**0.26**	**0.40**	**0.45**	**0.77**

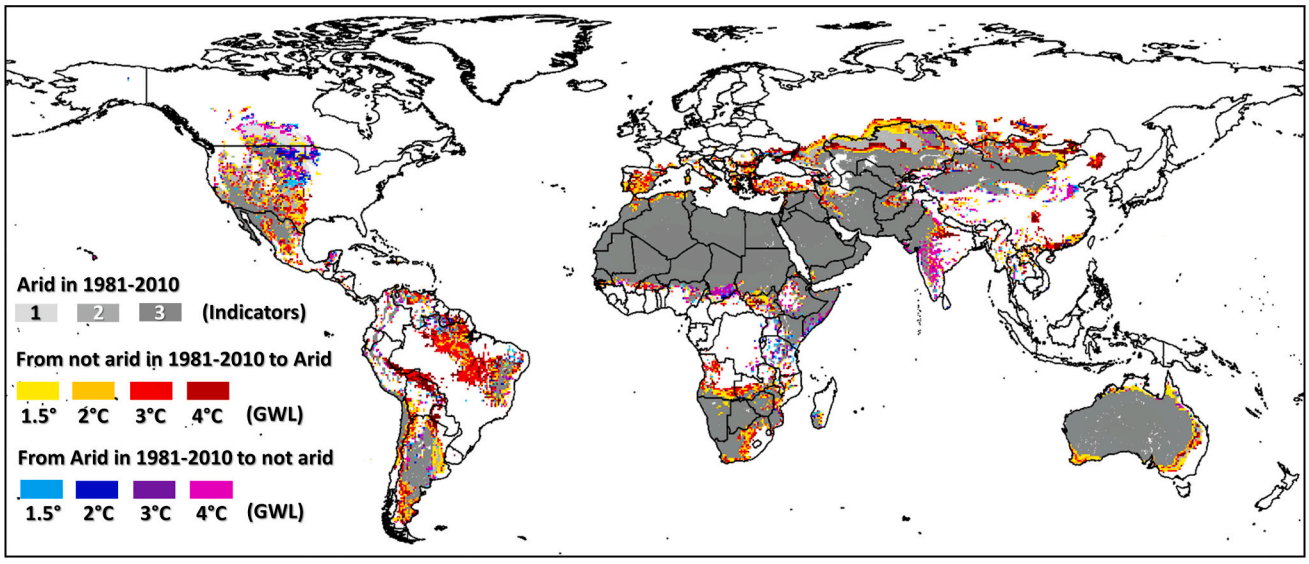

Fig. 1. Areas turning from not arid in 1981–2010 to arid at GWLs and from arid in 1981–2010 to not arid at GWLs.

2°C towards higher warming) and to peak at 4.4 billion with SSP3 at GWL 4°C (Fig. 3). The largest values correspond to SSP3 for most continents, exceeding 1.5 billion in Africa and 2 billion in Asia at GWL 4°C. However, in percentage (Table A5), the largest global values correspond to SSP4 (38.0% at GWL 3°C, starting from 24.6% in 1981–2010) and, at continental scale, to Europe (54.1% at GWL 4°C with SSP3). On the other hand, the population living in arid areas never exceeds 20% (with any SSP-GWL combination) in North America, there exceeding 100 million only with SSP5 at GWL 4°C.

The global population projected to face a shift towards arid climate (Fig. 4) never exceeds 130 million people at GWLs 1.5°C and 2°C with any SSP, but it notably increases at GWL 3°C, reaching approximately 330 million with SSP3, 270 million with SSP4, and 250 million with SSP5, and peaking at 500 million at GWL 4°C with SSP3 (around 330 million with SSP5). Most of these people are located in Asia and Africa where more than 100 million people are projected to face shifts towards arid climate under SSP3 from 3°C, with SSP4 from 3°C for Africa, and with SSP5 from 4°C for Asia. In percentage (Table S5), the continents with largest values are South America and Europe at both low and high GWLs and Central America at high GWLs (>10% with any SSP able to reach GWL 3°C).

With more sustainable SSPs (SSP1 and SSP2), the global population living in areas where arid areas are projected to retreat is very small, also because with these SSPs, few areas show projected increase in precipitation large enough to cause a shift towards wetter climate classes. With SSP4 the total number is about 130 million at GWL 3°C, and about 420 and 240 million at GWL 4°C respectively for SSP3 and SSP5 (Fig. 4). At global scale, population in areas facing a retreat of arid areas almost balances the population living in areas likely to turn arid at GWL 4°C, peaking at 3.4% of total population with SSP3 at GWL 4°C (Table A5) and being even larger in Asia (up to 4.7% with both SSP3 and SSP5 at GWL 4°C).

Focusing at the highest GWL for each SSP (Table 2), a few macro-regions stand out with more than 50 million people exposed to future shifts towards arid climate: the Mediterranean region (SSP3 and SSP5), south-eastern Africa (SSP3 and SSP4), eastern Asia (SSP3 and SSP5), and southern Asia (SSP3). In some regions, the population in areas turning from arid in 1981–2010 to not-arid in the future is larger than the population in areas experiencing the opposite pattern: north-western North America (SSP3, SSP4, and SSP5), western Africa (SSP3 and SSP5), central-eastern Africa (all SSPs), central Africa (SSP2), central Asia (SSP3 and SSP5), Tibetan Plateau (SSP3, SSP4, and SSP5), eastern Asia (SSP1 and SSP4), and southern Asia (all SSPs but SSP1).

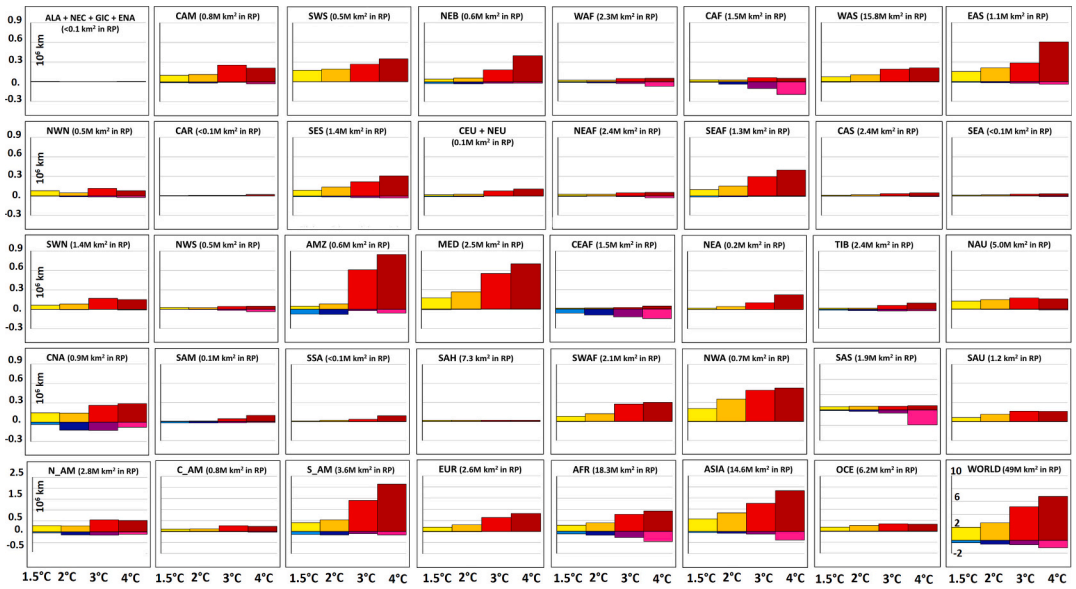

Fig. 2. Areas (10^6 km^2) turning from not arid in 1981–2010 to arid at four GWLs (yellow to dark red) and from arid in 1981–2010 to not-arid at four GWLs (light blue to purple). Values for macro-regions, continents, and global land follow different scales (see vertical axis of first panel for each type). See Fig. A2 for macro-regions and continents.

3.3. Land-use exposed to drying climate and enlargement of arid areas

Fig. 5 shows that, in the recent past, relevant extents of croplands were already in arid areas, in particular in the Northern Hemisphere. This is no surprise as many types of crops grow in semi-arid and arid areas (Creswell and Martin, 1998; Turner, 2004). However, in North America, Europe, Asia, and Oceania, the extent of croplands in arid areas show small changes between recent past and future GWLs (under any SSP). Instead, we found a remarkable increase of croplands in arid areas in Africa, especially with increasing warming under SSP3, with more than 3 million km^2 of African croplands (the 56%) likely to be in arid areas at GWL 4°C.

Globally, the largest extent of croplands in arid areas refers to SSP3, while this is likely to occur with both SSP3 and SSP4 for pastures, mostly in Africa, where sustainable grazing in arid grasslands is a key resource in many areas (Oba et al., 2000) and where (as in general in Southern Hemisphere), pastures and croplands are projected to notably enlarge with SSP3 and SSP4. For forests, this is likely to occur with SSP3 and SSP5, with the largest exposure in South America (>1 million km^2 already at GWL 3°C), where massive exploitation of resources in forested areas is not limited to Amazonia (Kirby et al., 2006; Costa and Pires, 2010), but also occurs in southern arid regions (Hoyos et al., 2013).

Croplands, pastures, and forested areas are likely to face a significant decrease in annual total precipitation with increasing GWLs, in particular from 3°C warming. With SSP3, at GWL 4°C, such a condition is projected for approximately 16% of global croplands, 14% of pastures, and 5% of forested areas (Table A6), respectively corresponding to 3.2 million km^2 of croplands, 1.2 million km^2 of pastures, and 1.7 million km^2 of forests (Fig. A8). Croplands are the most exposed class with any SSP in Europe and Oceania, whereas forests are the most exposed class in South America and Asia. In Northern and Central America and in Africa the role of the SSP is of highest importance.

Croplands show a progressively larger exposure to shifts to arid climates in all continents but North and Central America. This is the case also for pastures (excluding also Oceania) but with smaller absolute values. Forested areas, instead, show not negligible fractions exposed to enlargement of arid areas only in Asia and South America: however, in the latter continent such extent is above 0.5 million km^2 with any SSP from 3°C warming, representing the maximum exposure for a single class in a single continent (Fig. 6). Globally, the exposure to shifts towards arid climates is small for forested areas at low GWLs (<0.5% with any SSP at 2°C warming), while croplands and pastures, excluding SSP1, respectively show values above 2% and 3% at GWL 2°C (Table A6). The worst-case scenario, in percentage, is SSP5 for croplands (6.7% at GWL 4°C) and pastures (6.8% at GWL 4°C), and SSP3 for forests (3.6°C at GWL 4°C).

On the other hand, the shift from arid (in the past) to not-arid is likely to affect less than 0.3% of forests with any SSP-GWL combination (Table A6), and larger values for croplands and pastures, namely, up to 1.7% for pastures with SSP3 and SSP5 (at GWL 4°C) and 2.7% for croplands with SSP5 (at GWL 4°C). At global scale, no land-use class analyzed in this study shows an exposure to decreasingly arid conditions larger than an exposure to increasingly arid conditions. However, at continental scale there are few exceptions (Fig. 6), though in all cases the differences are very small: croplands in North America and Africa at GWL 2°C with SSP2, SSP3, and SSP4, pastures in Africa at GWL 2°C with SSP2, SSP3, and SSP4, and forests in South America at GWL 1.5° (but not at higher GWLs) with any SSP.

Regarding the selected land-use classes, at the highest GWL under SSP3, SSP4, or SSP5, the shift to arid climates is likely to involve an extent at least twice as large as with either SSP1 or SSP2 in all continents excluding Oceania for pastures, in Africa for croplands, and in South America for forests (Table 3). Moreover, the gap between the best-case and the worst-case scenarios can be very large: globally, the extent of pastures within areas that are likely to turn arid with SSP5 is four times larger than that with SSP1, that of croplands is three times larger (SSP5 versus SSP1), and that of forested areas twelve times larger with SSP3 than with SSP1.

3.4. A special focus on the SSP5

To investigate on a specific future, we selected the combination between RCP8.5 and SSP5, because, according to the specifics of the last generation of scenarios, the SSP5 is closely connected with RCP8.5 (O'Neill et al., 2014) and more than half of the simulations used in this study are based on RCP8.5. Moreover, the RCP8.5 is the worst-case scenario for climate hazards (Diffenbaugh and Giorgi, 2012) and we assume that this will help to better visualize the most severe consequences of climate change.

In a World following RCP8.5-SSP5, the continuous temperature

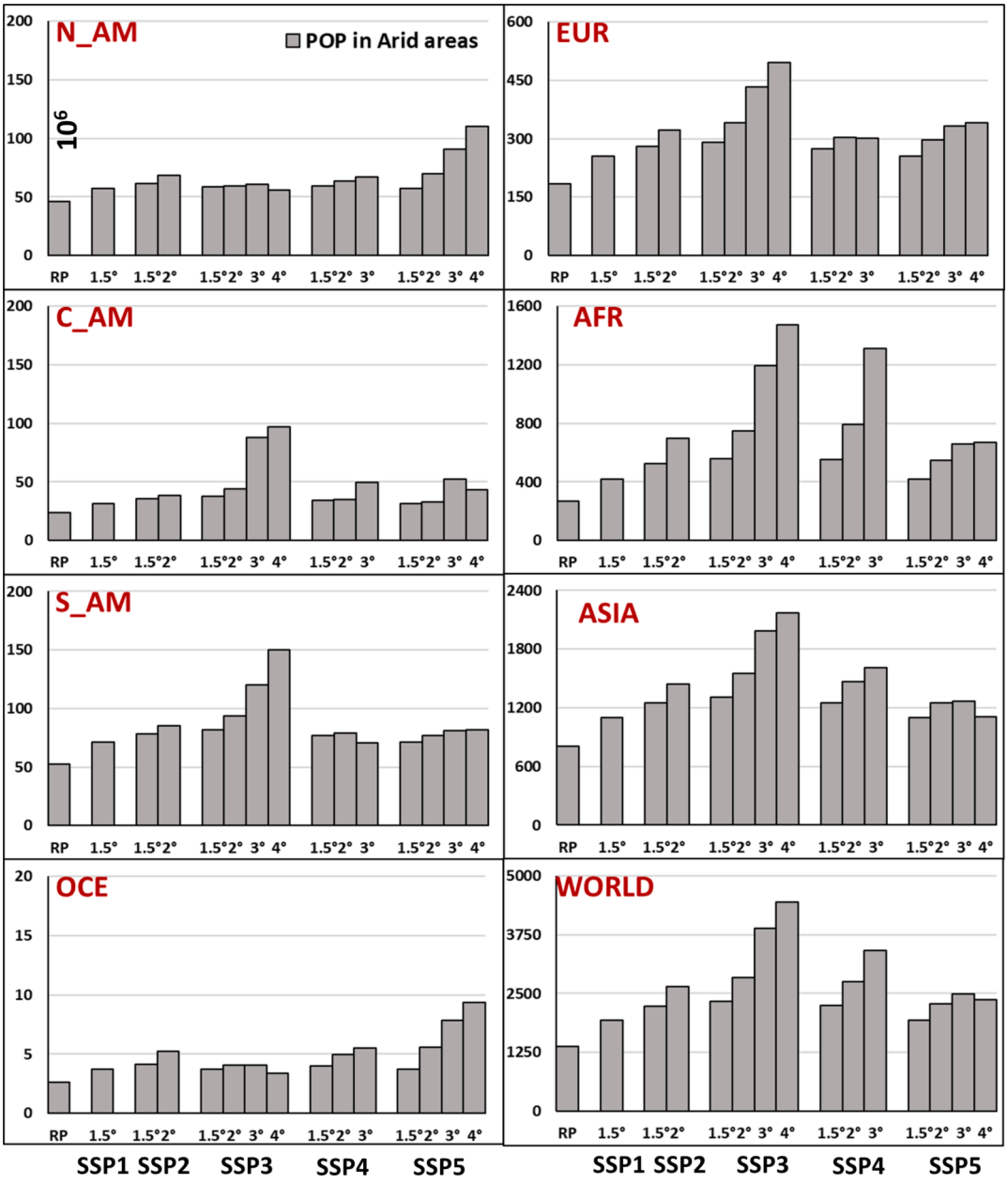

Fig. 3. Population (vertical axis: 10^6 people) living in arid areas in 1981–2010 (RP) and at GWLs from 1.5°C to 4°C. Values follow different scales for most continents.

increase and drying patterns (Fig. 7) are lead drivers of the progressive exposure to shifts towards arid climates. Even under stringent mitigation measures (global warming limited to 1.5°C), more than 50% of population will be exposed to significant precipitation decrease in south-western South America and the Mediterranean area, while this is likely to occur in central America and the Caribbean only at GWL 3°C, and in south-western Africa, northern and southern Australia at GWL 4°C. Consequently, in south-western South America more than 10% of population will live in areas likely to shift into arid areas already at 1.5°C warming, and the same conditions are likely to occur at GWL 3°C in central America, Amazonia, the Mediterranean region, south-eastern Africa, and north-western Asia, and at GWL 4°C in southern South America, south-western Africa, and north-eastern Africa (Fig. 8).

Oppositely, there are regions where less than 1% of people will be exposed to significant precipitation decrease even at high GWLs: regions at high latitudes in the Northern Hemisphere or at tropical latitudes in Africa and Asia. In some of these regions, i.e. north-western North America and central-eastern Africa (at GWL 3°C) and southern Asia (at GWL 4°C), more than 5% of the population is likely to live in areas shifting towards less arid climates (Fig. 8). In absolute values, the largest number of people experiencing this condition refers to southern Asia at GWL 4°C (around 140 million people; Table A7).

Regarding land-use, under the RCP8.5-SSP5 combination, the significant drying is projected to involve large fractions of pastures only at 3°C warming (especially Mexico and subtropical Africa). Forests will be subjected to significant drying in Chile, south-eastern China, and over the Pyrenees in Europe already at 1.5°C warming but, starting from GWL 3°C, wider areas will be involved, including central America, the European Alps, and Congo river basin. Regarding croplands, the Mediterranean region and southern Australia show progressive enlargement of areas exposed to significant drying with increasing GWL, and croplands will be exposed to such drying from 3°C warming also over parts of Mexico and southern Africa.

In most continents, croplands or pastures or both are likely to face

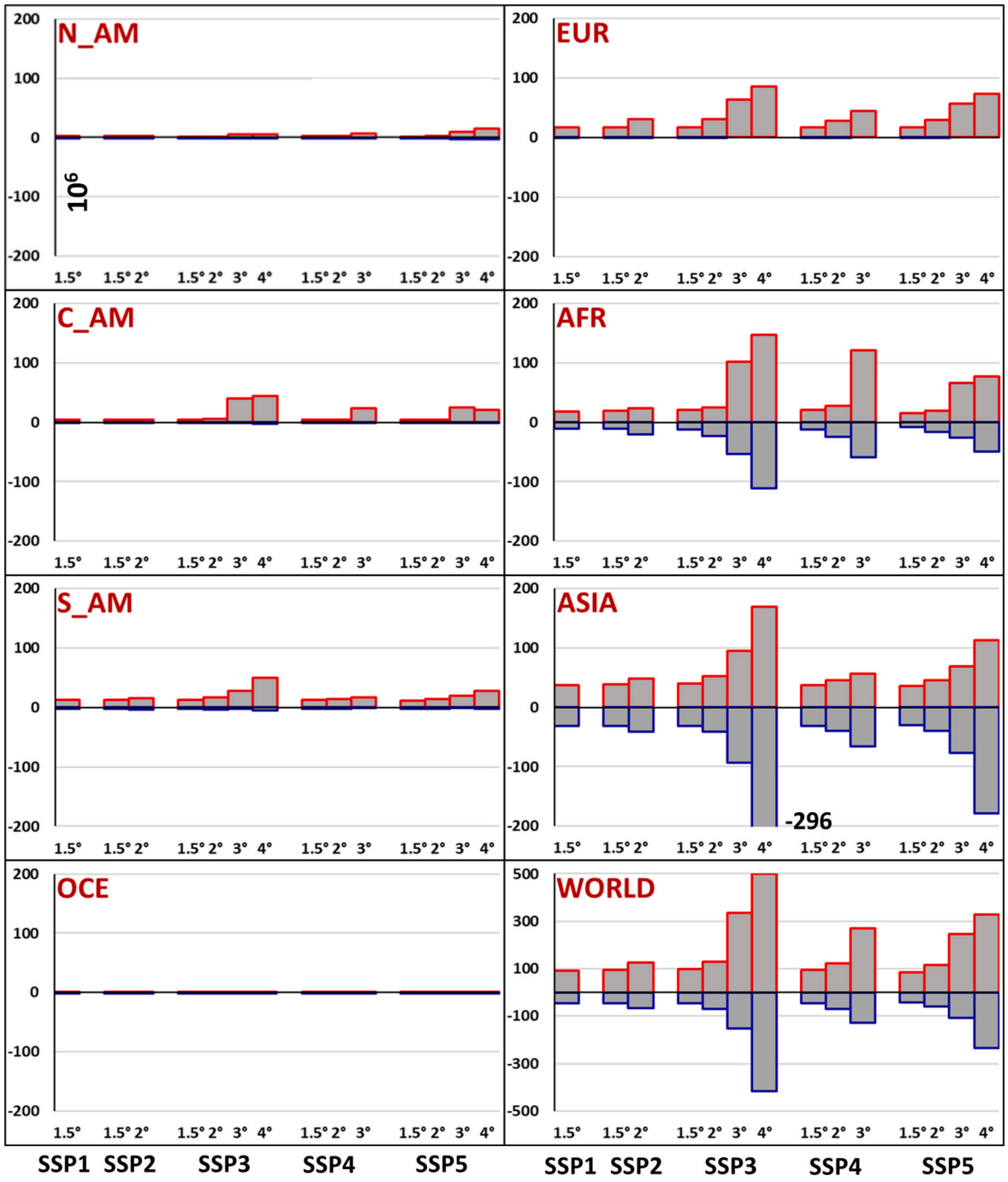

Fig. 4. Population (vertical axis: 10^6 people) in areas projected to turn from not arid in 1981–2010 into arid at four GWLs (red borders) and from arid in 1981–2010 to not arid at four GWLs (blue borders). For a better visualization of small values, we limited vertical axis to -200·10^6 and 200·10^6, but Asia shows larger negative values with SSP3-GWL4 (-296·10^6).

shift towards arid climates for more than 10% of their extent, while for forests this is likely to occur only in Amazonia (from GWL 3°C) with a maximum extent of 0.8 million km^2 of forests exposed at GWL 4°C (Table S8). More in detail (Fig. 9), 10% exposure is reached for pastures at GWL 1.5°C in north-western Asia, at 2°C in the Mediterranean region, at 3°C in south-western North America, south-western South America, Amazonia, south-western Africa, and western Asia, and at 4°C in central-northern North America, central America, and north-eastern Asia. 10% exposure is first reached for croplands in north-western Asia (GWL 1.5°C), then in southern Australia (2°C), then in central America, Amazonia, Mediterranean region, south-western Africa (3°C), and lastly in North-eastern Brazil, south-Eastern Africa, north-eastern and western Asia (4°C).

Small (for croplands) or very small (for pastures and forests) fractions of land-use are projected to be in areas where the arid areas are likely to retreat: at the highest GWL, around 0.5 million km^2 of croplands at global scale and around just 0.1 million km^2 of pastures and forests (Table A8). The 10% exposure to retreat of arid areas retreat is never reached in any macro-region, while the 5% is instead reached for croplands at GWL 2°C in central North America and central-eastern Africa, for pastures at GWL 4°C in central and central-eastern Africa, and southern Asia, and for forests at GWL 4°C in central-eastern Africa (Fig. 9). Such 5% is not reached anymore at GWL 4°C in central North America, despite progressive wetting, because of the projected reduction

Table 2
Left columns: population (10^6 people) living in arid areas in 1981–2010 (RP) and at highest GWL for each SSP. Central and right columns: population projected to live in areas which turned from not arid in 1981–2010 to arid at highest GWL for each SSP and in areas which turned from arid in 1981–2010 to not arid at highest GWL for each SSP. See Fig. A2 for macro-regions.

POP (10^6)	Arid						Not Arid to Arid					Arid to not Arid				
SSP		SSP1	SSP2	SSP3	SSP4	SSP5	SSP1	SSP2	SSP3	SSP4	SSP5	SSP1	SSP2	SSP3	SSP4	SSP5
REGION	RP	1.5°	2°	4°	3°	4°	1.5°	2°	4°	3°	4°	1.5°	2°	4°	3°	4°
A_N_G_E	0.0	0.0	0.0	0.0	0.0	0.0	0.0	0.0	0.0	0.0	0.0	0.0	0.0	0.0	0.0	0.0
NWN	3.1	4.0	4.7	2.0	3.0	5.3	0.1	0.1	0.1	0.1	0.2	0.0	0.0	1.0	1.5	2.6
SWN	39.0	47.9	57.7	46.7	54.5	86.9	1.0	0.9	1.6	1.4	4.0	0.0	0.1	0.1	0.0	0.2
CNA	3.9	5.4	5.7	7.5	9.6	18.0	1.0	1.1	4.3	5.5	10.5	0.2	0.7	0.3	0.7	0.8
CAM	23.2	31.0	37.6	95.1	48.9	43.1	3.8	4.4	43.4	23.9	20.3	0.6	0.5	2.3	0.1	1.1
CAR	0.5	0.8	0.9	1.6	0.8	0.6	0.1	0.2	0.3	0.1	0.1	0.0	0.0	0.0	0.0	0.0
NWS	17.3	24.2	28.5	43.3	22.7	21.0	2.0	2.1	4.6	2.9	2.0	0.1	0.5	1.9	0.5	0.8
SAM	0.5	0.6	1.0	2.0	1.2	0.6	0.1	0.4	0.7	0.4	0.2	0.2	0.2	0.3	0.2	0.1
SSA	0.0	0.0	0.0	0.1	0.0	0.0	0.0	0.0	0.1	0.0	0.0	0.0	0.0	0.0	0.0	0.0
SWS	3.8	10.9	12.8	20.4	9.7	12.9	6.5	7.4	13.2	5.7	8.9	0.0	0.0	0.0	0.0	0.0
SES	10.7	12.0	13.4	29.2	10.6	15.3	2.8	3.2	14.3	3.1	7.5	0.0	0.2	0.5	0.3	0.3
AMZ	11.8	16.0	20.7	41.6	20.2	23.9	0.5	1.1	11.5	3.6	6.5	1.3	1.8	1.1	0.1	0.6
NEB	8.0	7.6	8.6	13.2	5.9	8.3	0.5	0.8	4.8	1.0	3.0	0.5	0.5	1.4	0.3	0.9
N_CEU	12.3	14.6	16.7	17.8	13.7	25.1	3.0	6.2	9.9	5.9	13.2	0.3	0.6	0.0	0.0	0.0
MED	170.9	240.4	304.7	478.6	286.6	314.8	14.1	23.9	75.1	39.0	60.6	0.6	0.1	0.0	0.0	0.0
SAH	41.5	50.1	68.2	94.1	75.5	67.7	0.0	0.0	0.0	0.0	0.0	0.0	0.0	0.0	0.0	0.0
WAF	65.5	118.9	226.1	554.8	494.8	213.6	6.6	5.7	21.6	17.0	8.5	2.0	4.2	30.6	11.4	14.0
NEAF	57.8	98.1	159.0	290.3	275.5	136.2	3.1	6.2	10.9	16.0	5.7	0.3	0.3	5.6	1.3	2.7
CEAF	46.7	69.2	116.0	236.5	211.0	99.0	0.2	1.2	21.2	3.8	8.7	7.1	14.8	63.4	38.0	26.5
SWAF	8.5	12.0	17.0	32.1	25.5	20.5	0.3	0.8	9.6	6.8	4.7	0.3	0.0	0.0	0.0	0.0
SEAF	28.5	41.6	57.9	155.5	121.0	71.7	7.0	9.2	65.7	51.9	32.8	0.3	0.6	1.0	1.5	0.4
CAF	18.0	31.5	52.4	108.4	108.9	60.5	1.0	0.7	18.2	25.2	16.1	0.3	1.1	10.8	6.5	5.7
NEA	1.8	2.1	2.3	3.8	1.9	3.1	0.2	0.5	1.7	0.5	1.4	0.0	0.0	0.0	0.0	0.0
NWA	6.0	7.9	12.4	20.0	12.0	14.8	1.7	5.7	11.8	7.1	9.0	0.0	0.0	0.0	0.0	0.0
WAS	135.8	194.9	272.6	473.1	386.4	249.4	2.8	3.8	12.3	9.3	7.2	1.1	0.1	0.0	0.0	0.0
CAS	148.2	211.4	312.4	598.2	499.2	241.8	0.4	2.0	6.2	4.2	2.1	0.4	0.4	6.4	0.3	2.8
TIB	40.7	49.4	55.9	67.3	38.5	41.5	0.1	0.1	0.6	0.1	0.4	0.1	0.1	5.2	0.8	2.3
EAS	76.5	84.8	83.5	106.8	43.2	88.4	10.4	14.4	76.1	11.6	62.8	11.8	11.5	35.6	11.9	31.7
SAS	392.9	540.2	692.6	894.2	622.6	463.3	20.9	20.9	56.3	22.8	28.0	17.5	27.9	247.8	52.2	140.7
SEA	5.6	6.7	6.6	9.2	5.3	6.0	0.7	0.9	3.2	1.3	2.0	0.6	0.9	1.5	0.4	1.0
NAU	0.3	0.4	0.5	0.3	0.5	0.9	0.0	0.0	0.0	0.1	0.1	0.0	0.0	0.0	0.0	0.0
SAU	2.3	3.3	4.7	3.1	5.0	8.5	0.1	0.4	0.3	0.5	0.9	0.1	0.1	0.0	0.0	0.0
WORLD	1381.8	1937.9	2653.1	4446.8	3414.2	2362.8	91.3	124.3	499.4	270.9	327.5	45.6	67.5	416.8	128.1	235.1

of croplands in North America at high GWLs under SSP5.

Our results show that, similarly to SSP3 and SSP4, for SSP5 there are large differences between limited (GWLs 1.5°C and 2°C), medium (3°C), and large (4°C) population and land-use exposure to shifts towards arid climates. These findings highlight the importance of implementing policies to limit the global warming to sustainable values (Meinshausen et al., 2009; Rogelj et al., 2016). Under the SSP5, some regions stand out as hotspots, with more than 10% of population and of at least one of the analyzed land-use classes exposed: south-western South America already at GWL 1.5°C, central America, Amazonia, the Mediterranean region, and north-western Asia at GWL 3°C, and southwestern and south-eastern Africa, and north-eastern Asia only at GWL 4°C. Amongst these regions, one furtherly stands out, that is Amazonia, with more than 10% of population, croplands, pastures, and forests exposed to climatological shift to arid climates at GWLs 3°C and 4°C.

4. Discussion

According to the CORDEX simulations used in this study, future climate change implies a worldwide continuous temperature increase and spatially heterogeneous tendencies for precipitation (Table A2). Where total precipitation is likely to significantly decrease, the combined effect of drying and warming could lead to climate feedbacks, resulting in a shift towards semi-arid or arid conditions. Such shift is likely to be accelerated over areas that already suffered warming and drying in the recent past, as south-western South America, north-eastern Brazil, the Mediterranean region, mid-latitudes Asiatic steppe, southern South Africa, and southern Australia (Greve et al., 2014; Spinoni et al., 2015; Zarch et al., 2015).

According to our analyses, climate change is likely to put in danger of becoming arid (Table 1) a global total of 2.0 million km^2 of land at GWL 1.5°C, 2.7 million km^2 at GWL 2°C, 5.2 million km^2 at GWL 3°C, and 6.8 million km^2 at GWL 4°C. The continents with the largest areas in such conditions are Asia at low GWLs and South America at high GWLs, in particular eastern Amazonia (as reported by Marengo et al., 2012), a situation that can possibly be accelerated by feedbacks induced by deforestation (Paiva et al., 2020; Stabile et al., 2020).

Oppositely, the total area prone to retreat of arid climate ranges from 0.4 million km^2 at GWL 1.5°C to 1.2 million km^2 at GWL 4°C, in any case less than 0.8% of the global land. The two continents with the largest area prone to climate shifts from arid to not-arid are South America at GWL 1.5°C and Africa at high GWLs, in particular the Sahel region. Our findings seem to extend the recent debated Sahel greening into 21st century (Giannini et al., 2008; Dardel et al., 2014). CO_2 fertilization was reported to be the primary driver of recent greening and increased vegetation productivity over the tropics (Zhu et al., 2016; Lian et al., 2021), so it is likely that the projected high CO_2 emissions at high GWLs, together with increasing precipitation, could sustain the greening over central Africa.

No continent is likely to see a positive net balance between areas shifting from arid in the past to not arid in the future and vice-versa and the global extent of arid areas is projected to increase from 33.0% in 1981–2010 to 36.8% at GWL 4°C. This does not exclude future global greening, because our methodology does not focus at (further) greening over areas not classified as arid in 1981–2010. The ensemble CORDEX simulations used in this study projects a slight overall tendency to global wetting (Spinoni et al., 2021) and this – together with progressive increase of CO_2 and despite the warming – could lead to (further)

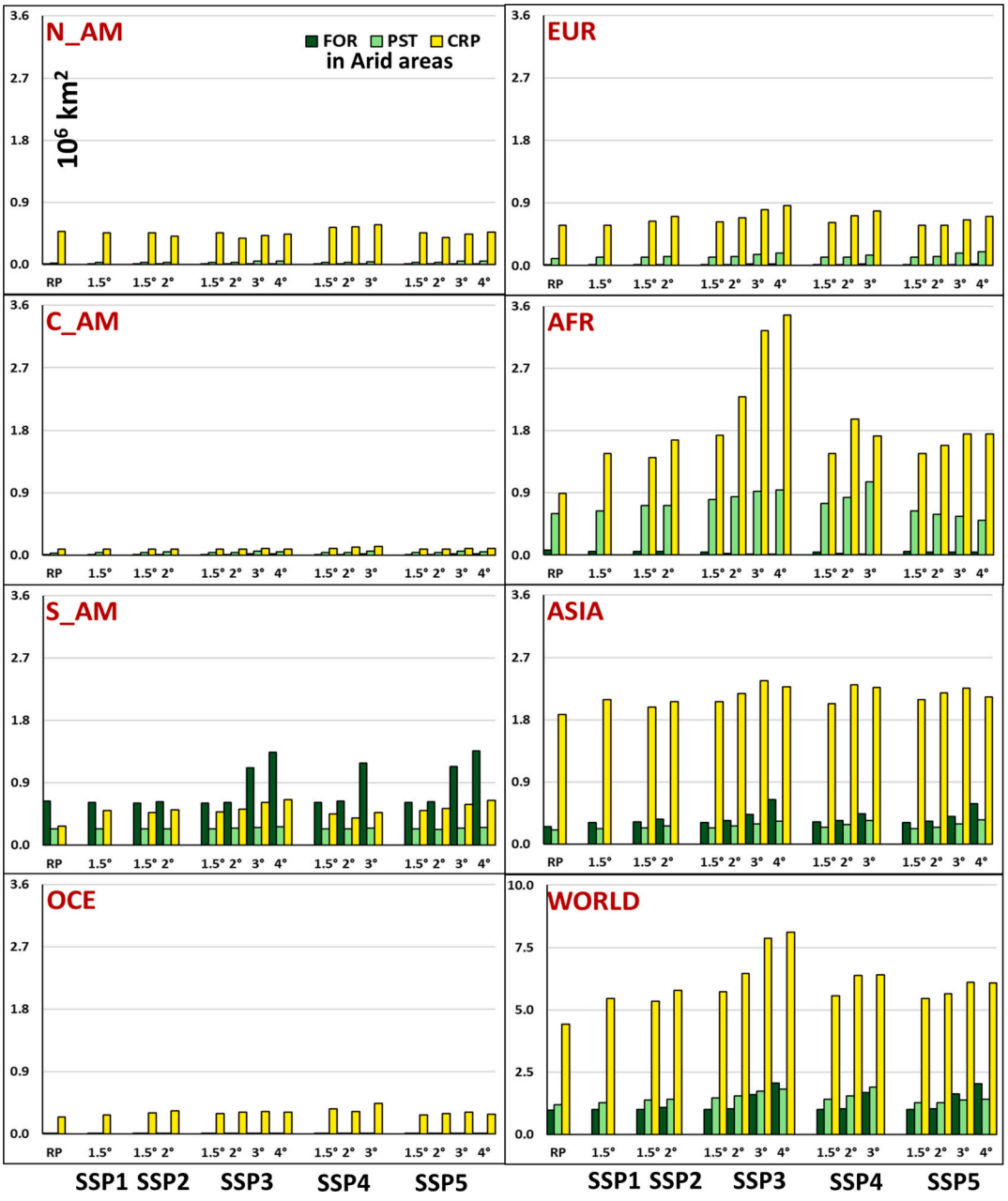

Fig. 5. As in Fig. 3, but for forests, pastures, and croplands (10^6 km^2).

greening, for example over boreal forests at northern latitudes (Piao et al., 2020).

The amount of population likely of being in areas projected to turn arid decisively depends on the development road that the World will take and, though global population is projected to be larger in 2100 than in the recent past with all SSPs, such an increase follows a very different curve depending on the SSP (Samir and Lutz, 2017). At continental scale, the inter-SSP differences play a key role: the largest increase would occur with SSP3 in Central and South America, Africa, and Asia, and with SSP5 in North America, Europe, and Oceania. Also land-use projections critically depend on the SSP (Popp et al., 2017), with typical local features, as for example forests in Brazil, with a projected increase with SSP4, decrease with SSP1, SSP3, and SSP5, and mixed patterns with SSP2 (Hurtt et al., 2020).

Combining climate and socio-economic projections, we found that in a World following green growth (SSP1) or middle-of-the-road (SSP2) scenarios, thus trying to follow the recommendations of the United Nations' Agenda 2030 (UN General Assembly, 2015), small fractions of population and land-use will be in areas shifting from not-arid to arid (Figs. 3–6). If, therefore, actions able to limit the temperature increase to 2°C warming (versus pre-industrial era) are taken, the advance of arid areas will be very limited and so the impacts on people and resources. Otherwise, with SSP3 and SSP5, but also with SSP4, the human and land-use capitals will be highly exposed to the effects of progressive drying and climate shift into arid conditions. With SSP3 and SSP5, by the end of 21st century an area of approximately 0.5 million km^2 for pastures and of 1.2 million km^2 for croplands and forests (each) will face concrete possibility of being in areas turned arid (Table 3 and Fig. 6). Furthermore, with SSP3 at GWL 4°C, around 500 million people will be in areas that shifted from not arid in recent past to arid and up to 4.5 billion people will be in arid areas (Table 3 and Figs. 3–4), which can also have effect on migratory fluxes (McLeman, 2014).

On the positive side, due to a wetting tendency over some regions with a 4°C warming, approximately 420 million people will be located

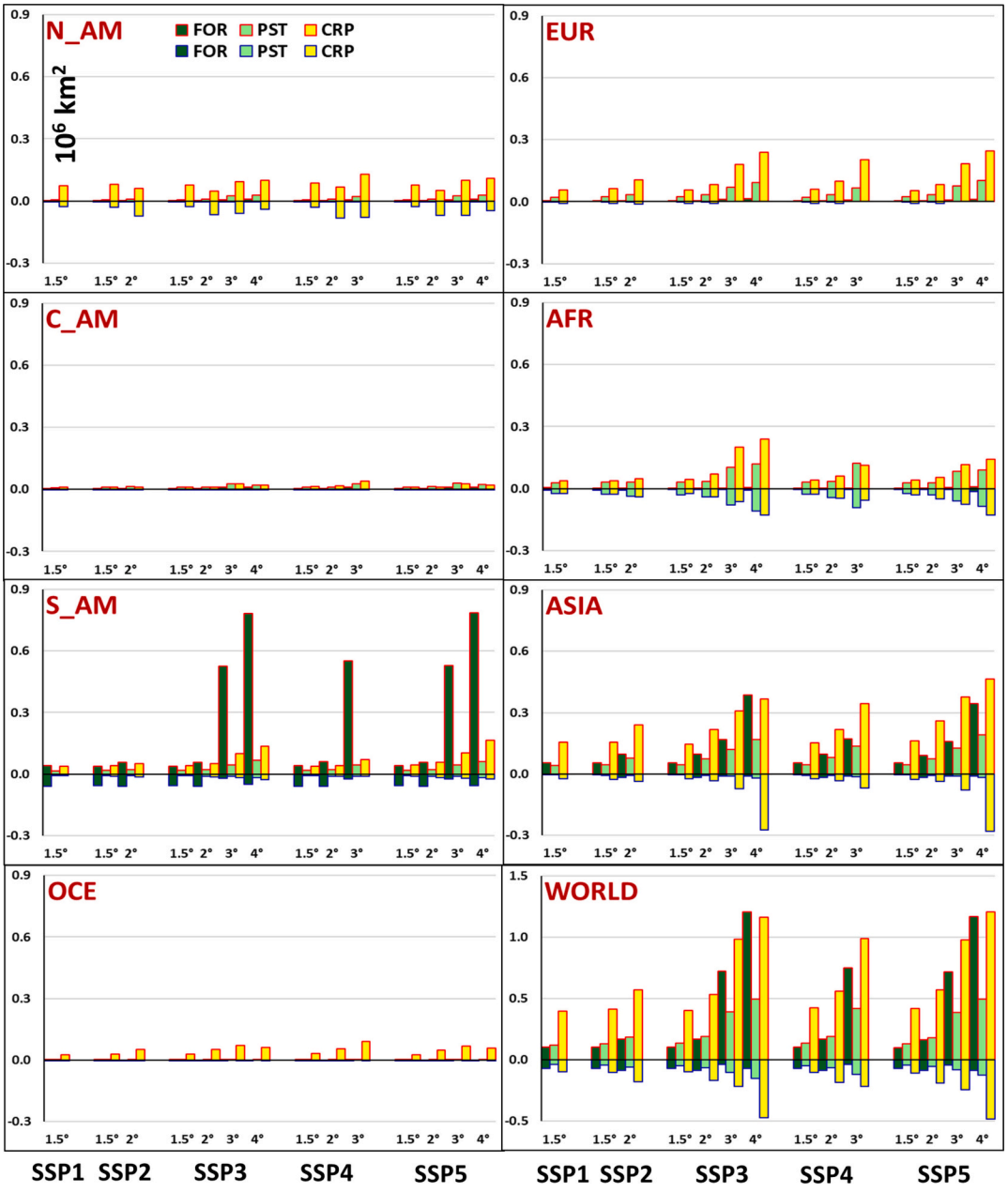

Fig. 6. As in Fig. 4 but for forests, pastures, and croplands (10^6 km^2).

in areas turned from arid in recent past into not arid with SSP3, and 240 million with SSP5, mostly over tropical latitudes in Africa and Asia (Table 3 and Fig. 4). Instead, the only land-use class that would partly benefit from warming-wetting tendency is croplands (Table 3 and Fig. 6), with approximately 0.5 million km^2 with SSP3 and SSP5 (at GWL 4°C) in areas where arid areas are likely to retreat in 21st century, in particular in Asia and Africa. Consequently, good policies could plan extending croplands in sustainable areas with positive impacts (Zabel et al., 2019).

The results shown in this study rely on aridity indices fully driven by atmospheric variables, so they can only describe the development of drylands from a climatological perspective and the effect of land–atmosphere coupling is only partially represented in our assessment. Atmospheric aridity is different from eco-hydrological aridity: the former, mainly driven by global warming (via increased temperature, vapor pressure deficit, and atmospheric demand of water), does not necessarily propagate to exacerbate the runoff and to force soil moisture deficit (Lian et al., 2021). As climate indicators do not account for components of the vegetation cycle as CO_2 fertilization and land-atmosphere feedbacks important for vegetation physiology (Berg and McColl, 2021), we compared our results to those by other surface-based indicators (soil moisture, runoff, and Leaf Area Index) to investigate possible overestimations of drylands.

Dealing with soil moisture, our results agree with those reported by Cheng et al. (2017) and Joo et al. (2020): future hotspots of drying are the Mediterranean Region, north-eastern and southwestern South America, southern Africa, southwestern and eastern U.S., and Australia. Moreover, as we showed in Section 3, Joo et al. (2020) reported that soil moisture depletion in such hotspots is projected to increase with increasing GWL.

Instead, our projections show increasing aridity at mid-latitudes in Asia and those based on total soil moisture show wetting tendency at mid-latitudes in Northern Hemisphere (Berg et al., 2017). This depends on the inaccurate estimation of the total soil water availability by

Table 3
As in Table 2 but for pastures, croplands, and forests (10^6 km^2).

Land-Use		Arid						Not Arid to Arid					Arid to Not Arid				
(10^6 km^2)	SSP		SSP1	SSP2	SSP3	SSP4	SSP5	SSP1	SSP2	SSP3	SSP4	SSP5	SSP1	SSP2	SSP3	SSP4	SSP5
CLASS	REG	*RP*	1.5°C	2°C	4°C	3°C	4°C	1.5°C	2°C	4°C	3°C	4°C	1.5°C	2°C	4°C	3°C	4°C
	N_AM	*0.02*	0.03	0.03	0.05	0.04	0.05	0.01	0.01	0.03	0.02	0.03	0.00	0.00	0.00	0.00	0.00
	C_AM	*0.03*	0.04	0.05	0.05	0.06	0.05	0.01	0.01	0.02	0.03	0.02	0.00	0.00	0.00	0.00	0.00
	S_AM	*0.23*	0.23	0.23	0.27	0.25	0.26	0.02	0.02	0.07	0.04	0.06	0.01	0.01	0.02	0.01	0.02
Pastures	**EUR**	*0.10*	0.12	0.13	0.18	0.15	0.20	0.02	0.03	0.09	0.07	0.10	0.00	0.00	0.00	0.00	0.00
	AFR	*0.60*	0.64	0.72	0.94	1.06	0.51	0.03	0.03	0.12	0.12	0.09	0.02	0.04	0.11	0.09	0.09
	ASIA	*0.20*	0.22	0.26	0.33	0.34	0.35	0.04	0.08	0.17	0.14	0.19	0.00	0.01	0.02	0.01	0.02
	OCE	*0.00*	0.00	0.00	0.01	0.00	0.00	0.00	0.00	0.00	0.00	0.00	0.00	0.00	0.00	0.00	0.00
	WORLD	*1.20*	1.29	1.43	1.83	1.90	1.42	0.12	0.18	0.49	0.42	0.50	0.04	0.06	0.15	0.12	0.13
	N_AM	*0.48*	0.46	0.41	0.44	0.58	0.47	0.07	0.06	0.10	0.13	0.11	0.03	0.07	0.04	0.08	0.05
	C_AM	*0.09*	0.09	0.09	0.09	0.13	0.09	0.01	0.01	0.02	0.04	0.02	0.00	0.00	0.00	0.00	0.00
	S_AM	*0.28*	0.50	0.51	0.66	0.47	0.65	0.04	0.05	0.13	0.07	0.16	0.01	0.01	0.03	0.01	0.02
Croplands	**EUR**	*0.58*	0.58	0.71	0.86	0.79	0.71	0.06	0.11	0.24	0.20	0.25	0.01	0.01	0.00	0.00	0.00
	AFR	*0.89*	1.47	1.66	3.47	1.73	1.75	0.04	0.05	0.24	0.11	0.14	0.02	0.04	0.13	0.06	0.13
	ASIA	*1.87*	2.09	2.06	2.28	2.27	2.13	0.15	0.24	0.37	0.34	0.47	0.02	0.04	0.27	0.07	0.28
	OCE	*0.24*	0.27	0.34	0.31	0.44	0.28	0.03	0.05	0.06	0.09	0.06	0.00	0.00	0.00	0.00	0.00
	WORLD	*4.43*	5.46	5.77	8.12	6.40	6.08	0.40	0.57	1.16	0.99	1.21	0.10	0.18	0.47	0.22	0.48
	N_AM	*0.00*	0.01	0.01	0.01	0.01	0.01	0.00	0.00	0.01	0.01	0.01	0.00	0.00	0.00	0.00	0.00
	C_AM	*0.01*	0.01	0.01	0.02	0.02	0.02	0.00	0.00	0.01	0.01	0.01	0.00	0.00	0.00	0.00	0.00
	S_AM	*0.64*	0.61	0.63	1.34	1.19	1.36	0.04	0.06	0.78	0.55	0.79	0.06	0.06	0.05	0.03	0.06
Forests	**EUR**	*0.01*	0.01	0.01	0.03	0.02	0.02	0.00	0.01	0.01	0.01	0.01	0.00	0.00	0.00	0.00	0.00
	AFR	*0.07*	0.05	0.05	0.02	0.01	0.04	0.00	0.00	0.00	0.00	0.01	0.01	0.01	0.01	0.00	0.01
	ASIA	*0.25*	0.31	0.36	0.65	0.44	0.59	0.05	0.10	0.39	0.17	0.34	0.00	0.02	0.01	0.01	0.01
	OCE	*0.00*	0.00	0.00	0.00	0.00	0.00	0.00	0.00	0.00	0.00	0.00	0.00	0.00	0.00	0.00	0.00
	WORLD	*0.98*	1.00	1.08	2.06	1.69	2.05	0.10	0.17	1.21	0.75	1.17	0.07	0.09	0.07	0.04	0.08

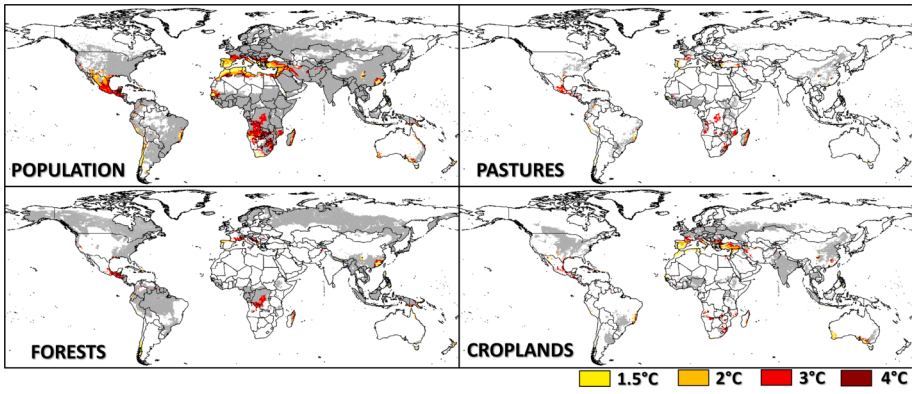

Fig. 7. Population and land-use classes progressively exposed to significant precipitation decrease from 1981–2010 to four GWLs under SSP5 scenario. In grey, areas (populated or covered by the corresponding land-use class) not affected by significant precipitation decrease.

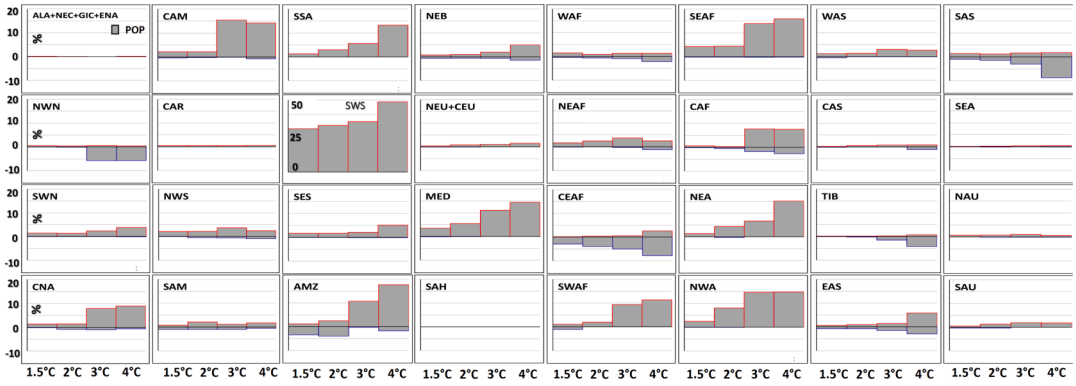

Fig. 8. Macro-regional percentage (%) of population in areas projected to turn from not arid in 1981–2010 into arid at GWLs (red borders) and from arid in 1981–2010 to not arid at GWLs (blue borders), according to SSP5. Vertical axis for south-western South America (SWS) is different than all other regions. See Fig. A2 for macro-regions.

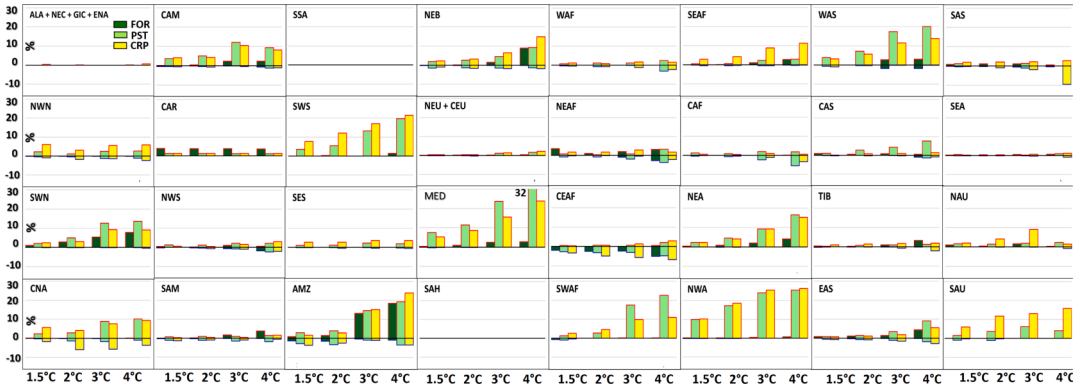

Fig. 9. As in Fig. 8 but for forests, pastures, and croplands.

climate indicators, which instead tend to show projections of aridity in line (though they show overall larger values) with those of surface soil moisture (Berg et al., 2017).

We highlight that current and past generations of Earth System Models show high uncertainty in dry areas either trying to estimate soil moisture when compared to observations (Berg and Sheffield, 2018) and in soil moisture projections, with smaller uncertainties in wet regions (Cheng et al., 2017). In drylands, soil moisture feedbacks could help regulating evapotranspiration and atmospheric moisture, possibly reducing the decrease in soil water content, but the robust modeling of this process is difficult because of the high inter-model variability (Zhou et al., 2021).

Dealing with runoff indicators, the global drying trends projected by climate models and reported in scientific literature seem in contradiction with runoff projections, which show future increase at global scale (Milly and Dunne, 2016; Greve et al., 2019). Climate models do not incorporate the increased water use by vegetation with high CO_2 concentration, thus they potentially overestimate drying compared to runoff simulations, despite the latter show high variability and remarkable uncertainties (Lehner et al., 2019). However, though at global scale our projections show increasing arid areas, the results of our study overall agree with runoff projections reported by Yang et al. (2019), which indicate the Mediterranean region, eastern China, sparse areas in South America and in the United States, and sub-Saharan Africa as the areas likely to face the most severe drying in the 21st century.

Dealing with eco-hydrological indexes, our projections of aridity do not agree with a recent study based on an ensemble of Dynamic Global Vegetation Models (DGVMs), which reported no future expansion of global drylands (Berg and McColl, 2021). Such divergence likely reflects different index sensitivities to hydro-climate change and responses to the physiological effect on vegetation of increasing atmospheric CO_2.

DGVMs include vegetation properties as key prognostic variables and their interactions with surface biophysics, hydrology and biogeochemistry are represented through equations of varying complexity (Piao et al., 2013). Land surface processes, such as changes in vegetation and land-atmosphere interactions, can have an important role in modulating further water-stress conditions and DGVMs can therefore explicitly reproduce key features of terrestrial water cycle and are undoubtedly valuable tools to explore land-atmosphere interactions and their effect of aridity. DGVMs include the effects of increasing CO_2, which leads to increase in efficiency of plant water use and can reduce ecohydrological aridity because of increase in biomass and reduction of water limitations (Berg and McColl, 2021). DGVMs include vegetation indicators as LAI (Fang et al., 2019), which allows evaluating interannual variations in vegetation, which may exert a strong control on climate, particularly during extreme events such as meteorological droughts and heatwaves (Forzieri et al., 2020). Such vegetation-mediated processes could become even more relevant in view of the projected increase LAI across most of the globe (Mahowald et al., 2016).

However, DGVMs have shown limitations in reproducing the interplay between vegetation and climate due to an incomplete understanding and model representation of some biophysical processes (Duveiller et al., 2018; Forzieri et al., 2018). Recently, a comparison of DGVM simulations and satellite retrievals suggests that DGVMs tend to overestimate the sensitivity to CO_2 and underestimate the biophysical response of ecosystems to changes in water availability (Forzieri et al., 2020). In addition, LAI is subject to the high variability of ESM models (Mahowald et al., 2016) and may overestimate future vegetation trends and underestimate drying (Berg and McColl, 2021). Consequently, results based on eco-hydrological indexes derived from DGVMs, though they can more comprehensively represent the underlying physical processes, can – on the other hand – potentially underestimate the future development of drylands.

The emerging contrasting patterns in future scenarios of global drylands areas emphasize the need of further studies to reconcile these findings and derive conclusive statements about the role of land–atmosphere coupling in affecting the development of future arid and semi-arid areas. Drylands are complex system and are likely to respond non-linearly to future evolution of climate, also due to the interactions between ecosystems, hydrological cycle, and human activities as well as enhanced future risks to droughts and heatwaves (Lian et al., 2021).

Additionally, drylands are the largest source of interannual variability in global carbon sink and play a key role in future variability of vegetation productivity at global scale (Yao et al., 2020). Consequently, a better understanding of the evolution of drylands can help reducing the large uncertainties (Schlund et al., 2020) in the projected increase of gross and net primary production forced by both warming and increasing CO_2 (Anav et al., 2015; Campbell et al., 2017; Cai and Prentice, 2020).

5. Conclusions

In this study, we started from the methodology described in Spinoni et al. (2015) and applied in the 3rd edition of WAD (Cherlet et al., 2018), to delineate future changes in arid areas, this time using a combination of three – instead of two – indicators. The use of the FAO-UNEP aridity index, the Köppen-Geiger climate classification, and the Holdridge life zones, allowed detecting the areas likely to becoming arid, with general agreement with those reported by Fu and Feng (2014), Roderick et al. (2015), Zarch et al. (2015), and Lin et al. (2018), with small-scale differences in particular over North America (specifically Mexico) due to a refined delineation thanks to RCMs.

Our results show that the most important hotpots are: the bordering areas between the United States and Mexico (reported also by Seager et al., 2007), north-eastern Brazil (see Marengo and Bernasconi, 2015), southern Argentina (see Fernandez et al., 2019), the Mediterranean region (see Gao and Giorgi, 2008), western and southern African drylands (see Platts et al., 2015, and Sylla et al., 2016), central Asia (see

Lioubimtseva and Henebry, 2009, and Poonia and Rao, 2013), sparse areas in China (see Chan et al., 2016, and Wang et al., 2017), and semi-arid areas in Australia (see Greve and Seneviratne, 2015).

Overall, around 1.8% of global lands will turn into arid areas if warming is limited to 2°C; instead, at GWL4°C, around 4.6% of lands will shift from not arid to arid. This results in increasing fractions of population and land-use likely to be within arid areas, with crucially dependency on the type of socio-economic development: for sustainable scenarios (SSP1 and SSP2), in the 21st century less than 130 million people will face a concrete possibility to live in areas that shifted to arid climates; for more severe scenarios (SSP3, SSP4, and SSP5), more than 270 million people will face such possibility (0.5 billion with SSP3), in particular in Africa and Asia. With respect to population in arid areas, our results for the special combination RCP8.5-SSP5 overall agree with those reported by Koutroulis (2019), based on one climate model only, with very similar spatial patterns and slightly larger differences at high GWLs.

At continental scale, such a shift towards arid climates is projected to affect large forested areas in South America, pastures mostly in Europe, Asia, and Africa, and large croplands especially in the Northern Hemisphere. Regarding forests, our findings agree with literature for Asia (Liu et al., 2013; Zhang et al., 2013) and represent a novelty for South America. About croplands, our results confirm that, in a warming future, those in semi-arid areas will be almost everywhere in danger (Sivakumar et al., 2005; Dimes et al., 2008; Jacobsen et al., 2012). At the time of writing and based on our knowledge, no studies on future global exposure of pastures to the drying climate are available as comparison.

The use of three indicators to delineate the future arid areas is one of the highlights of this study. As the arbitrary choice of such indicators and the harmonization of their thresholds can be regarded as a drawback, adding other indicators is an option that should be evaluated with care. Economic and population growth can suffer from water scarcity, so the use of climate indicators to delineate arid lands can be effective in a rapidly changing future (Lian et al., 2021), but there is large room for improvements. The investigation of future population and land-use classes exposed to drying should aim at including both atmospheric and ecohydrological aridity, by means of indicators accounting for soil moisture, runoff, vegetation status and productivity, CO_2 effect on land surface, and so on (Berg and McColl, 2021).

The results shown in this paper will be part of the European Commission's Global Drought Observatory (GDO; see https://edo.jrc.ec.europa.eu/gdo/). Stakeholders, land managers, and governments could use them when implementing policies and conservation measures to mitigate progressive land degradation (Stringer et al., 2007; Fleskens and Stringer, 2014), hence preventing desertification, cope with it, or adapt to its consequences (Bisaro et al., 2014; Chasek et al., 2015). In particular, our results could be used to help achieving Goal 13 (Climate Action) and Goal 15 (Life on land) of the United Nations' Sustainabile Development Goals, with the latter aiming at combating desertification, halting and reversing land degradation and biodiversity loss, by promoting sustainable use and management of terrestrial ecosystems (UN General Assembly, 2015; see also: https://sdgs.un.org/goals).

According to our results, limiting the global warming below the 2°C threshold could limit the advance of arid areas but, in order to combat desertification, politicians and scientists have to take action at many levels (Bauer and Stringer, 2009; Huang et al., 2020), from local interventions to avoid the excessive exploitation of land resources (Schwilch et al., 2009; Cowie et al., 2018) to structured transnational monitoring and assessment of land degradation (Vogt et al., 2011). However, if no effective actions will be implemented, an uncontrolled drying of semi-arid and arid areas could dramatically impact croplands and pastures and cause food crisis or famine (Smith et al., 2020) and lead to poverty (Way, 2016), in particular in less developed countries (Sachs, 2007; Tschakert, 2007; Johnson et al., 2016), and eventually force mass migration (Leighton, 2006; Rechkemmer, 2009; Bettini and Andersson, 2014).

Data availability

The input CORDEX climate data can be found at one of the Earth System Grid Federation's (ESGF) websites, e.g.: https://esg-dn1.nsc.liu.se/projects/esgf-liu/. The observed climate data can be found at the DWD's website (https://www.dwd.de/EN/ourservices/gpcc/gpcc.html; GPCC) and at the University of East Anglia's website (https://sites.uea.ac.uk/cru/data/; CRU).

The projected population data can be found at NASA-SEDAC's website: https://sedac.ciesin.columbia.edu/data/set/popdynamics-1-8th-pop-base-year-projection-ssp-2000-2100-rev01/data-download). The projected land-use data can be found at the LUH2's website: https://luh.umd.edu/.

The population and land-use future exposure to meteorological droughts under five SSPs will be included in the European Commission's Global Drought Observatory (https://edo.jrc.ec.europa.eu/gdo/php/index.php?id=2001).

Disclaimer

This research did not receive any specific grant from funding agencies in the public, commercial, or not-for-profit sectors.

Declaration of Competing Interest

The authors declare that they have no known competing financial interests or personal relationships that could have appeared to influence the work reported in this paper.

Appendix A. Supplementary data

Supplementary data to this article can be found online at https://doi.org/10.1016/j.gloplacha.2021.103597.

References

Adamo, S.B., Crews-Meyer, K.A., 2006. Aridity and desertification: exploring environmental hazards in Jáchal, Argentina. Appl. Geogr. 26 (1), 61–85.
Alexander, P., Prestele, R., Verburg, P.H., Arneth, A., Baranzelli, C., Batista e Silva, F., Doelman, J.C., 2017. Assessing uncertainties in land cover projections. Glob. Chang. Biol. 23 (2), 767–781.
Allen, R.G., Pereira, L.S., Raes, D., Smith, M., 1998. Crop evapotranspiration-Guidelines for computing crop water requirements-FAO Irrigation and drainage paper 56. Fao, Rome 300 (9), D05109.
Alvares, C.A., Stape, J.L., Sentelhas, P.C., de Moraes, G., Leonardo, J., Sparovek, G., 2013. Köppen's climate classification map for Brazil. Meteorol. Z. 22 (6), 711–728.
Anav, A., Friedlingstein, P., Beer, C., Ciais, P., Harper, A., Jones, C., Zhao, M., 2015. Spatiotemporal patterns of terrestrial gross primary production: A review. Rev. Geophys. 53 (3), 785–818.
Batibeniz, F., Ashfaq, M., Diffenbaugh, N.S., Key, K., Evans, K.J., Turuncoglu, U.U., Önol, B., 2020. Doubling of US Population Exposure to Climate Extremes by 2050. Earth's Future 8 (4).
Bauer, S., Stringer, L.C., 2009. The role of science in the global governance of desertification. J. Environ. Dev. 18 (3), 248–267.
Beck, H.E., Zimmermann, N.E., McVicar, T.R., Vergopolan, N., Berg, A., Wood, E.F., 2018. Present and future Köppen-Geiger climate classification maps at 1-km resolution. Sci. data 5, 180214.
Belda, M., Holtanová, E., Halenka, T., Kalvová, J., 2014. Climate classification revisited: from Köppen to Trewartha. Clim. Res. 59 (1), 1–13.
Berg, A., McColl, K.A., 2021. No projected global drylands expansion under greenhouse warming. Nat. Clim. Chang. 11 (4), 331–337.
Berg, A., Sheffield, J., 2018. Soil moisture–evapotranspiration coupling in CMIP5 models: Relationship with simulated climate and projections. J. Clim. 31 (12), 4865–4878.
Berg, A., de Noblet-Ducoudré, N., Sultan, B., Lengaigne, M., Guimberteau, M., 2013. Projections of climate change impacts on potential C4 crop productivity over tropical regions. Agric. For. Meteorol. 170, 89–102.
Berg, A., Findell, K., Lintner, B., Giannini, A., Seneviratne, S.I., Van Den Hurk, B., Cheruy, F., 2016. Land–atmosphere feedbacks amplify aridity increase over land under global warming. Nat. Clim. Chang. 6 (9), 869–874.
Berg, A., Sheffield, J., Milly, P.C., 2017. Divergent surface and total soil moisture projections under global warming. Geophys. Res. Lett. 44 (1), 236–244.
Bestelmeyer, B.T., Okin, G.S., Duniway, M.C., Archer, S.R., Sayre, N.F., Williamson, J.C., Herrick, J.E., 2015. Desertification, land use, and the transformation of global drylands. Front. Ecol. Environ. 13 (1), 28–36.

Bettini, G., Andersson, E., 2014. Sand waves and human tides: exploring environmental myths on desertification and climate-induced migration. J. Environ. Dev. 23 (1), 160–185.
Bisaro, A., Kirk, M., Zdruli, P., Zimmermann, W., 2014. Global drivers setting desertification research priorities: insights from a stakeholder consultation forum. Land Degrad. Dev. 25 (1), 5–16.
Bradley, A.V., Rosa, I.M., Brandão, A., Crema, S., Dobler, C., Moulds, S., Ewers, R.M., 2017. An ensemble of spatially explicit land-cover model projections: prospects and challenges to retrospectively evaluate deforestation policy. Model. Earth Syst. Environ. 3 (4), 1215–1228.
Cai, W., Prentice, I.C., 2020. Recent trends in gross primary production and their drivers: analysis and modelling at flux-site and global scales. Environ. Res. Lett. 15 (12), 124050.
Calvin, K., Bond-Lamberty, B., Clarke, L., Edmonds, J., Eom, J., Hartin, C., McJeon, H., 2017. The SSP4: a world of deepening inequality. Glob. Environ. Chang. 42, 284–292.
Campbell, J.E., Berry, J.A., Seibt, U., Smith, S.J., Montzka, S.A., Launois, T., Laine, M., 2017. Large historical growth in global terrestrial gross primary production. Nature 544 (7648), 84–87.
Chan, D., Wu, Q., Jiang, G., Dai, X., 2016. Projected shifts in Köppen climate zones over China and their temporal evolution in CMIP5 multi-model simulations. Adv. Atmos. Sci. 33 (3), 283–293.
Chasek, P., Safriel, U., Shikongo, S., Fuhrman, V.F., 2015. Operationalizing zero net land degradation: The next stage in international efforts to combat desertification? J. Arid Environ. 112, 5–13.
Chen, X., Zhang, X.S., Li, B.L., 2003. The possible response of life zones in China under global climate change. Glob. Planet. Chang. 38 (3–4), 327–337.
Cheng, S., Huang, J., Ji, F., Lin, L., 2017. Uncertainties of soil moisture in historical simulations and future projections. J. Geophys. Res.-Atmos. 122 (4), 2239–2253.
Cherlet, M., Hutchinson, C., Reynolds, J., Hill, J., Sommer, S., von Maltitz, G. (Eds.), 2018. World Atlas of Desertification. Publication Office of the European Union, Luxembourg.
Colantoni, A., Ferrara, C., Perini, L., Salvati, L., 2015. Assessing trends in climate aridity and vulnerability to soil degradation in Italy. Ecol. Indic. 48, 599–604.
Colwell, R.K., Brehm, G., Cardelús, C.L., Gilman, A.C., Longino, J.T., 2008. Global warming, elevational range shifts, and lowland biotic attrition in the wet tropics. Science 322 (5899), 258–261.
Cook, B.I., Smerdon, J.E., Seager, R., Coats, S., 2014. Global warming and 21st century drying. Clim. Dyn. 43 (9–10), 2607–2627.
Costa, M.H., Pires, G.F., 2010. Effects of Amazon and Central Brazil deforestation scenarios on the duration of the dry season in the arc of deforestation. Int. J. Climatol. 30 (13), 1970–1979.
Cowie, A.L., Orr, B.J., Sanchez, V.M.C., Chasek, P., Crossman, N.D., Erlewein, A., Tengberg, A.E., 2018. Land in balance: The scientific conceptual framework for Land Degradation Neutrality. Environ. Sci. Pol. 79, 25–35.
Creswell, R., Martin, F.W., 1998. Dry land farming: Crops & Techniques for arid regions. ECHO technical note, Fort Myers, Fl, USA.
Crosbie, R.S., Pollock, D.W., Mpelasoka, F.S., Barron, O.V., Charles, S.P., Donn, M.J., 2012. Changes in Köppen-Geiger climate types under a future climate for Australia: hydrological implications. Hydrol. Earth Syst. Sci. 16 (9).
D'Odorico, P., Bhattachan, A., Davis, K.F., Ravi, S., Runyan, C.W., 2013. Global desertification: drivers and feedbacks. Adv. Water Resour. 51, 326–344.
D'Odorico, P., Rosa, L., Bhattachan, A., Okin, G.S., 2019. Desertification and land degradation. In: D'Odorico, P., Porporato, A., Wilkinson Runyan, C. (Eds.), Dryland Ecohydrology. Springer, Cham. https://doi.org/10.1007/978-3-030-23269-6_21.
Dardel, C., Kergoat, L., Hiernaux, P., Grippa, M., Mougin, E., Ciais, P., Nguyen, C.C., 2014. Rain-use-efficiency: What it tells us about the conflicting Sahel greening and Sahelian paradox. Remote Sens. 6 (4), 3446–3474.
Dell'Aquila, A., Mariotti, A., Bastin, S., Calmanti, S., Cavicchia, L., Deque, M., Gualdi, S., 2018. Evaluation of simulated decadal variations over the Euro-Mediterranean region from ENSEMBLES to Med-CORDEX. Clim. Dyn. 51 (3), 857–876.
Dendoncker, N., Schmit, C., Rounsevell, M., 2008. Exploring spatial data uncertainties in land-use change scenarios. Int. J. Geogr. Inf. Sci. 22 (9), 1013–1030.
Derguy, M.R., Frangi, J.L., Drozd, A.A., Arturi, M.F., Martinuzzi, S., 2019. Holdridge Life Zone Map: Republic of Argentina. Gen.Tech. Rep. 51.
Diffenbaugh, N.S., Giorgi, F., 2012. Climate change hotspots in the CMIP5 global climate model ensemble. Clim. Chang. 114 (3–4), 813–822.
Dimes, J.P., Cooper, P.J., Rao, K.P.C., 2008. Climate change impact on crop productivity in the semi-arid tropics of Zimbabwe in the 21st century. In: Proceedings of the Workshop on Increasing the Productivity and Sustainability of Rain-Fed Cropping Systems of Poor Smallholder Farmers, pp. 189–198.
Dosio, A., Fischer, E.M., 2018. Will half a degree make a difference? Robust projections of indices of mean and extreme climate in Europe under 1.5 C, 2 C, and 3 C global warming. Geophys. Res. Lett. 45 (2), 935–944.
Dosio, A., Jones, R.G., Jack, C., Lennard, C., Nikulin, G., Hewitson, B., 2019. What can we know about future precipitation in Africa? Robustness, significance and added value of projections from a large ensemble of regional climate models. Clim. Dyn. 53 (9–10), 5833–5858.
Dosio, A., Turner, A.G., Tamoffo, A.T., Sylla, M.B., Lennard, C., Jones, R.G., Hewitson, B., 2020. A tale of two futures: contrasting scenarios of future precipitation for West Africa from an ensemble of regional climate models. Environ. Res. Lett. 15 (6), 064007.
Dregne, H.E., 2002. Land degradation in the drylands. Arid Land Res. Manag. 16 (2), 99–132.
Duveiller, G., Forzieri, G., Robertson, E., Li, W., Georgievski, G., Lawrence, P., Wiltshire, A., Ciais, P., Pongratz, J., Sitch, S., Arneth, A., Cescatti, A., 2018. Biophysics and Vegetation Cover Change: A Process-Based Evaluation Framework for Confronting Land Surface Models with Satellite Observations. Earth System Science Data Discussions, pp. 1–24. https://doi.org/10.5194/essd-2018-24.
Elagib, N.A., Abdu, A.S.A., 1997. Climate variability and aridity in Bahrain. J. Arid Environ. 36 (3), 405–419.
El-Beltagy, A., Madkour, M., 2012. Impact of climate change on arid lands agriculture. Agric. Food Secur. 1 (1), 3.
Engelbrecht, C.J., Engelbrecht, F.A., 2016. Shifts in Köppen-Geiger climate zones over southern Africa in relation to key global temperature goals. Theor. Appl. Climatol. 123 (1–2), 247–261.
Evans, J.P., Di Virgilio, G., Hirsch, A.L., Hoffmann, P., Remedio, A.R., Ji, F., Coppola, E., 2020. The cordex-australasia ensemble: evaluation and future projections. Clim. Dyn. 1–17.
Fang, H., Baret, F., Plummer, S., Schaepman-Strub, G., 2019. An overview of global leaf area index (LAI): methods, products, validation, and applications. Rev. Geophys. 57 (3), 739–799.
Feng, S., Fu, Q., 2013. Expansion of global drylands under a warming climate. Atmos. Chem. Phys. 13 (10), 081-10.
Feng, H., Zhang, M., 2015. Global land moisture trends: drier in dry and wetter in wet over land. Sci. Rep. 5 (1), 1–6.
Fensholt, R., Langanke, T., Rasmussen, K., Reenberg, A., Prince, S.D., Tucker, C., Epstein, H., 2012. Greenness in semi-arid areas across the globe 1981–2007—an Earth Observing Satellite based analysis of trends and drivers. Remote Sens. Environ. 121, 144–158.
Fernandez, J.P., Franchito, S.H., Rao, V.B., 2019. Future changes in the aridity of South America from regional climate model projections. Pure Appl. Geophys. 176 (6), 2719–2728.
Feser, F., Rockel, B., von Storch, H., Winterfeldt, J., Zahn, M., 2011. Regional climate models add value to global model data: a review and selected examples. Bull. Am. Meteorol. Soc. 92 (9), 1181–1192.
Finkel, J.M., Canel-Katz, L.M., Katz, J.I., 2016. Decreasing US aridity in a warming climate. Int. J. Climatol. 36 (3), 1560–1564.
Fleskens, L., Stringer, L.C., 2014. Land management and policy responses to mitigate desertification and land degradation. Land Degrad. Dev. 25 (1), 1–4.
Forzieri, G., Duveiller, G., Georgievski, G., Li, W., Robertson, E., Kautz, M., Lawrence, P., Martin, L.G.S., Anthoni, P., Ciais, P., Pongratz, J., Sitch, S., Wiltshire, A., Arneth, A., Cescatti, A., 2018. Evaluating the interplay between biophysical processes and leaf area changes in land surface models. J. Adv. Model. Earth Syst. 10, 1102–1126. https://doi.org/10.1002/2018MS001284.
Forzieri, G., Miralles, D.G., Ciais, P., Alkama, R., Ryu, Y., Duveiller, G., Zhang, K., Robertson, E., Kautz, M., Martens, B., Jiang, C., Arneth, A., Georgievski, G., Li, W., Ceccherini, G., Anthoni, P., Lawrence, P., Wiltshire, A., Pongratz, J., Piao, S., Sitch, S., Goll, D.S., Arora, V.K., Lienert, S., Lombardozzi, D., Kato, E., Nabel, J.E.M. S., Tian, H., Friedlingstein, P., Cescatti, A., 2020. Increased control of vegetation on global terrestrial energy fluxes. Nat. Clim. Chang. 10, 356–362. https://doi.org/10.1038/s41558-020-0717-0.
Fricko, O., Havlik, P., Rogelj, J., Klimont, Z., Gusti, M., Johnson, N., Ermolieva, T., 2017. The marker quantification of the Shared Socioeconomic pathway 2: a middle-of-the-road scenario for the 21st century. Glob. Environ. Chang. 42, 251–267.
Fu, Q., Feng, S., 2014. Responses of terrestrial aridity to global warming. J. Geophys. Res.-Atmos. 119 (13), 7863–7875.
Fu, Q., Lin, L., Huang, J., Feng, S., Gettelman, A., 2016. Changes in terrestrial aridity for the period 850–2080 from the Community Earth System Model. J. Geophys. Res.-Atmos. 121 (6), 2857–2873.
Fujimori, S., Hasegawa, T., Masui, T., Takahashi, K., Herran, D.S., Dai, H., Kainuma, M., 2017. SSP3: AIM implementation of shared socioeconomic pathways. Glob. Environ. Chang. 42, 268–283.
Fujioka, T., Chappell, J., 2010. History of Australian aridity: chronology in the evolution of arid landscapes. Geol. Soc. Lond., Spec. Publ. 346 (1), 121–139.
Gao, X., Giorgi, F., 2008. Increased aridity in the Mediterranean region under greenhouse gas forcing estimated from high resolution simulations with a regional climate model. Glob. Planet. Chang. 62 (3-4), 195–209.
Geiger, R., 1954. Klassifikation der klimate nach W. Köppen. *Landolt-Börnstein–Zahlenwerte und Funktionen aus Physik, Chemie, Astronomie*. Geophysik und Technik 3, 603–607.
Geist, H., 2017. The causes and progression of desertification. In: Routledge Studies in Environmental Policy and Practice, 1 edition. Routledge. February 8, 2005.
Geist, H.J., Lambin, E.F., 2004. Dynamic causal patterns of desertification. Bioscience 54 (9), 817–829.
Giannini, A., Biasutti, M., Verstraete, M.M., 2008. A climate model-based review of drought in the Sahel: desertification, the re-greening and climate change. Glob. Planet. Chang. 64 (3–4), 119–128.
Giorgi, F., Jones, C., Asrar, G.R., 2009. Addressing climate information needs at the regional level: the CORDEX framework. WMO Bull. 58 (3), 175.
Glantz, M.H., 2019. Desertification: environmental degradation in and around arid lands. CRC Press, Taylor and Francis, United States.
Grainger, A. (Ed.), 2015. The Threatening Desert: Controlling Desertification. Routledge. Editor: Taylor & Francis Ltd, United States. EAN: 9781138928862.
Greve, P., Seneviratne, S.I., 2015. Assessment of future changes in water availability and aridity. Geophys. Res. Lett. 42 (13), 5493–5499.
Greve, P., Orlowsky, B., Mueller, B., Sheffield, J., Reichstein, M., Seneviratne, S.I., 2014. Global assessment of trends in wetting and drying over land. Nat. Geosci. 7 (10), 716–721.
Greve, P., Roderick, M.L., Ukkola, A.M., Wada, Y., 2019. The aridity Index under global warming. Environ. Res. Lett. 14 (12), 124006.

Hansen, A.J., Neilson, R.P., Dale, V.H., Flather, C.H., Iverson, L.R., Currie, D.J., Bartlein, P.J., 2001. Global change in forests: responses of species, communities, and biomes: interactions between climate change and land use are projected to cause large shifts in biodiversity. BioScience 51 (9), 765–779.
Hansen, J., Ruedy, R., Sato, M., Lo, K., 2010. Global surface temperature change. Rev. Geophys. 48 (4).
Hargreaves, G.H., Samani, Z.A., 1985. Reference crop evapotranspiration from temperature. Appl. Eng. Agric. 1 (2), 96–99.
Harris, I., Osborn, T.J., Jones, P., Lister, D., 2020. Version 4 of the CRU TS monthly high-resolution gridded multivariate climate dataset. Sci. data 7 (1), 1–18.
Hawkins, E., Ortega, P., Suckling, E., Schurer, A., Hegerl, G., Jones, P., Thorne, P., 2017. Estimating changes in global temperature since the preindustrial period. Bull. Am. Meteorol. Soc. 98 (9), 1841–1856.
He, B., Wang, S., Guo, L., Wu, X., 2019. Aridity change and its correlation with greening over drylands. Agric. For. Meteorol. 278, 107663.
Hein, L., De Ridder, N., 2006. Desertification in the Sahel: a reinterpretation. Glob. Chang. Biol. 12 (5), 751–758.
Holdridge, L.R., Grenke, W.C., 1971. Forest Environments in Tropical Life Zones: A Pilot Study.
Holdridge, L.R., Tosi, J.A., 1967. *Life Zone Ecology* (No. 581.5 H727e ing). Centro Científico Tropical, San José, CR.
Hoyos, L.E., Cingolani, A.M., Zak, M.R., Vaieretti, M.V., Gorla, D.E., Cabido, M.R., 2013. Deforestation and precipitation patterns in the arid Chaco forests of central Argentina. Appl. Veg. Sci. 16 (2), 260–271.
Huang, J., Yu, H., Guan, X., Wang, G., Guo, R., 2016. Accelerated dryland expansion under climate change. Nat. Clim. Chang. 6 (2), 166–171.
Huang, J., Zhang, G., Zhang, Y., Guan, X., Wei, Y., Guo, R., 2020. Global desertification vulnerability to climate change and human activities. Land Degrad. Dev. 31 (11), 1380–1391.
Hughes, L., 2011. Climate change and Australia: key vulnerable regions. Reg. Environ. Chang. 11 (1), 189–195.
Huo, Z., Dai, X., Feng, S., Kang, S., Huang, G., 2013. Effect of climate change on reference evapotranspiration and aridity index in arid region of China. J. Hydrol. 492, 24–34.
Hurtt, G.C., Chini, L., Sahajpal, R., Frolking, S., Bodirsky, B.L., Calvin, K., Zhang, X., 2020. Harmonization of global land use change and management for the period 850–2100 (LUH2) for CMIP6. Geosci. Model Dev. 13 (11), 5425–5464.
Imeson, A., 2012. Desertification, Land Degradation and Sustainability. John Wiley & Sons, Chichester, West Sussex, United Kingdom.
IPCC, 2018. In: Masson-Delmotte, V., Zhai, P., Pörtner, H.O., Roberts, D., Skea, J., Shukla, P.R., Pirani, A., Moufouma-Okia, W., Péan, C., Pidcock, R., Connors, S., Matthews, J.B.R., Chen, Y., Zhou, X., Gomis, M.I., Lonnoy, E., Maycock, T., Tignor, M., Waterfield, T. (Eds.), 2018: Global Warming of 1.5°C. An IPCC Special Report on the Impacts of Global Warming of 1.5°C above Pre-Industrial Levels and Related Global Greenhouse Gas Emission Pathways, in the Context of Strengthening the Global Response to the Threat of Climate Change, Sustainable Development, and Efforts to Eradicate Poverty. World Meteorological Organization, Geneva, Switzerland.
Jacobsen, S.E., Jensen, C.R., Liu, F., 2012. Improving crop production in the arid Mediterranean climate. Field Crop Res. 128, 34–47.
Johnson, P.M., Mayrand, K., Paquin, M., 2016. The United Nations Convention to Combat Desertification in global sustainable development governance. In: Governing Global Desertification. Routledge, New York, US, pp. 21–30.
Jones, B., O'Neill, B.C., 2020. Global One-Eighth Degree Population Base Year and Projection Grids Based on the Shared Socioeconomic Pathways, Revision 01. Palisades. NASA Socioeconomic Data and Applications Center (SEDAC), NY. https://doi.org/10.7927/m30p-j498. Accessed 13 May 2020.
Joo, J., Jeong, S., Zheng, C., Park, C.E., Park, H., Kim, H., 2020. Emergence of significant soil moisture depletion in the near future. Environ. Res. Lett. 15 (12), 124048.
Jump, A.S., Penuelas, J., 2005. Running to stand still: adaptation and the response of plants to rapid climate change. Ecol. Lett. 8 (9), 1010–1020.
Kafle, H.K., Bruins, H.J., 2009. Climatic trends in Israel 1970–2002: warmer and increasing aridity inland. Clim. Chang. 96 (1–2), 63–77.
Kendon, E.J., Ban, N., Roberts, N.M., Fowler, H.J., Roberts, M.J., Chan, S.C., Wilkinson, J.M., 2017. Do convection-permitting regional climate models improve projections of future precipitation change? Bull. Am. Meteorol. Soc. 98 (1), 79–93.
Kirby, K.R., Laurance, W.F., Albernaz, A.K., Schroth, G., Fearnside, P.M., Bergen, S., Da Costa, C., 2006. The future of deforestation in the Brazilian Amazon. Futures 38 (4), 432–453.
Kniveton, D.R., Smith, C.D., Black, R., 2012. Emerging migration flows in a changing climate in dryland Africa. Nat. Clim. Chang. 2 (6), 444–447.
Knutti, R., Sedláček, J., 2013. Robustness and uncertainties in the new CMIP5 climate model projections. Nat. Clim. Chang. 3 (4), 369–373.
Köppen, W.D., 1936. Das geographische system der klimat. Handbuch der klimatologie 46.
Körner, C., Larcher, W., 1988. Plant life in cold climates. In: Symposia of the Society for Experimental Biology, Vol. 42, pp. 25–57.
Kottek, M., Grieser, J., Beck, C., Rudolf, B., Rubel, F., 2006. World map of the Köppen-Geiger climate classification updated. Meteorol. Z. 15 (3), 259–263.
Koutroulis, A.G., 2019. Dryland changes under different levels of global warming. Sci. Total Environ. 655, 482–511.
Krause, A., Haverd, V., Poulter, B., Anthoni, P., Quesada, B., Rammig, A., Arneth, A., 2019. Multimodel analysis of future land use and climate change impacts on ecosystem functioning. Earth's Future 7 (7), 833–851.
Kriegler, E., Bauer, N., Popp, A., Humpenöder, F., Leimbach, M., Strefler, J., Mouratiadou, I., 2017. Fossil-fueled development (SSP5): an energy and resource intensive scenario for the 21st century. Glob. Environ. Chang. 42, 297–315.
Legasa, M.N., Manzanas, R., Fernández, J., Herrera, S., Iturbide, M., Moufouma-Okia, W., Gutiérrez, J.M., 2020. Assessing multidomain overlaps and grand ensemble generation in CORDEX regional projections. Geophys. Res. Lett. 47 (4), e2019GL086799.
Lehner, F., Wood, A.W., Vano, J.A., Lawrence, D.M., Clark, M.P., Mankin, J.S., 2019. The potential to reduce uncertainty in regional runoff projections from climate models. Nat. Clim. Chang. 9 (12), 926–933.
Leighton, M., 2006. Desertification and migration. In: Johnson, P.M., Mayrand, K., Paquin, M. (Eds.), Governing global desertification: Linking Environmental Degradation, Poverty and Participation. Ashgate Publishing Group, Burlington, USA, pp. 63–78.
Lian, X., Piao, S., Chen, A., Huntingford, C., Fu, B., Li, L.Z., Roderick, M.L., 2021. Multifaceted characteristics of dryland aridity changes in a Warming World. Nat. Rev. Earth Environ. 1–19.
Lin, L., Gettelman, A., Fu, Q., Xu, Y., 2018. Simulated differences in 21st century aridity due to different scenarios of greenhouse gases and aerosols. Clim. Chang. 146 (3-4), 407–422.
Lioubimtseva, E., Henebry, G.M., 2009. Climate and environmental change in arid Central Asia: Impacts, vulnerability, and adaptations. J. Arid Environ. 73 (11), 963–977.
Liu, H., Park Williams, A., Allen, C.D., Guo, D., Wu, X., Anenkhonov, O.A., Badmaeva, N. K., 2013. Rapid warming accelerates tree growth decline in semi-arid forests of Inner Asia. Glob. Chang. Biol. 19 (8), 2500–2510.
Lugo, A.E., Brown, S.L., Dodson, R., Smith, T.S., Shugart, H.H., 1999. The Holdridge life zones of the conterminous United States in relation to ecosystem mapping. J. Biogeogr. 26 (5), 1025–1038.
Ma, L., Hurtt, G.C., Chini, L.P., Sahajpal, R., Pongratz, J., Frolking, S., Doelman, J.C., 2020. Global rules for translating land-use change (LUH2) to land-cover change for CMIP6 using GLM2. Geosci. Model Dev. 13 (7), 3203–3220.
Mahowald, N., Lo, F., Zheng, Y., Harrison, L., Funk, C., Lombardozzi, D., Goodale, C., 2016. Projections of leaf area index in earth system models. Earth Syst. Dynam. 7, 211–229. https://doi.org/10.5194/esd-7-211-2016.
Mainguet, M., 2002. Desertification: Natural Background and Human Mismanagement, 1st edition. Springer-Verlag, Berlin. 1991, 2nd edition 1994. Springer Science & Business Media.
Maliva, R., Missimer, T., 2012. Aridity and drought. In: Arid Lands Water Evaluation and Management. Springer, Berlin, Heidelberg, pp. 21–39.
Marengo, J.A., Bernasconi, M., 2015. Regional differences in aridity/drought conditions over Northeast Brazil: present state and future projections. Clim. Chang. 129 (1–2), 103–115.
Marengo, J.A., Chou, S.C., Kay, G., Alves, L.M., Pesquero, J.F., Soares, W.R., Chagas, D. J., 2012. Development of regional future climate change scenarios in South America using the Eta CPTEC/HadCM3 climate change projections: climatology and regional analyses for the Amazon, São Francisco and the Paraná River basins. Clim. Dyn. 38 (9-10), 1829–1848.
Martynov, A., Laprise, R., Sushama, L., Winger, K., Šeparović, L., Dugas, B., 2013. Reanalysis-driven climate simulation over CORDEX North America domain using the Canadian Regional Climate Model, version 5: model performance evaluation. Clim. Dyn. 41 (11), 2973–3005.
McLeman, R.A., 2014. Climate and Human Migration: Past Experiences, Future Challenges. Cambridge University Press, Cambridge (UK). ISBN: 9781107606708.
Meinshausen, M., Meinshausen, N., Hare, W., Raper, S.C., Frieler, K., Knutti, R., Allen, M. R., 2009. Greenhouse-gas emission targets for limiting global warming to 2 C. Nature 458 (7242), 1158–1162.
Mendizabal, T., Puigdefabregas, J., 2003. Population and land use changes: impacts on desertification in Southern Europe and in the Maghreb. In: Security and Environment in the Mediterranean. Springer, Berlin, Heidelberg, pp. 687–701.
Milly, P.C., Dunne, K.A., 2016. Potential evapotranspiration and continental drying. Nat. Clim. Chang. 6 (10), 946–949.
Moore, A.D., Ghahramani, A., 2013. Climate change and broadacre livestock production across southern Australia. Impacts of climate change on pasture and livestock productivity, and on sustainable levels of profitability. Glob. Chang. Biol. 19 (5), 1440–1455.
Moral, F.J., Rebollo, F.J., Paniagua, L.L., García-Martín, A., Honorio, F., 2016. Spatial distribution and comparison of aridity indices in Extremadura, southwestern Spain. Theor. Appl. Climatol. 126 (3–4), 801–814.
Mu, J.E., McCarl, B.A., Wein, A.M., 2013. Adaptation to climate change: changes in farmland use and stocking rate in the US. Mitig. Adapt. Strateg. Glob. Chang. 18 (6), 713–730.
Muhire, I., Ahmed, F., 2016. Spatiotemporal trends in mean temperatures and aridity index over Rwanda. Theor. Appl. Climatol. 123 (1-2), 399–414.
Neely, C., Bunning, S., Wilkes, A., 2009. Review of evidence on drylands pastoral systems and climate change. FAO Technical Papers, Rome, Italy.
Nickl, E., Millones, M., Parmentier, B., Lucatello, S., Trejo, A., 2020. Drylands, Aridification, and Land Governance in Latin America: a Regional Geospatial Perspective. In: Stewardship of Future Drylands and Climate Change in the Global South. Springer International Publishing, Cham, Switzerland, pp. 281–299.
O'Neill, B.C., Kriegler, E., Riahi, K., Ebi, K.L., Hallegatte, S., Carter, T.R., van Vuuren, D. P., 2014. A new scenario framework for climate change research: the concept of shared socioeconomic pathways. Clim. Chang. 122 (3), 387–400.
O'Neill, B.C., Kriegler, E., Ebi, K.L., Kemp-Benedict, E., Riahi, K., Rothman, D.S., Levy, M., 2017. The roads ahead: Narratives for shared socioeconomic pathways describing world futures in the 21st century. Glob. Environ. Chang. 42, 169–180.
Oba, G., Stenseth, N.C., Lusigi, W.J., 2000. New perspectives on sustainable grazing management in arid zones of sub-Saharan Africa. BioScience 50 (1), 35–51.

Pachauri, R.K., Allen, M.R., Barros, V.R., Broome, J., Cramer, W., Christ, R., Dubash, N. K., 2014. Climate Change 2014: Synthesis Report. Contribution of Working Groups I, II and III to the Fifth Assessment Report of the Intergovernmental Panel on Climate Change. Ipcc, p. 151.

Paiva, P.F.P.R., Ruivo, M.D.L.P., da Silva Junior, O.M., Maciel, M.D.N.M., Braga, T.G.M., de Andrade, M.M.N., Gama, L.H.O.M., 2020. Deforestation in protected areas in the Amazon: a threat to biodiversity. Biodivers. Conserv. 29 (1), 19–38.

Pearcy, R.W., Ehleringer, J., 1984. Comparative ecophysiology of C_3 and C_4 plants. Plant Cell Environ. 7 (1), 1–13.

Peel, M.C., Finlayson, B.L., Mcmahon, T.A., 2007. Updated world map of the Köppen-Geiger climate classification. Hydrol. Earth Syst. Sci. 11, 1633–1644.

Piao, S., Sitch, S., Ciais, P., Friedlingstein, P., Peylin, P., Wang, X., Ahlström, A., Anav, A., Canadell, J.G., Cong, N., Huntingford, C., Jung, M., Levis, S., Levy, P.E., Li, J., Lin, X., Lomas, M.R., Lu, M., Luo, Y., Ma, Y., Myneni, R.B., Poulter, B., Sun, Z., Wang, T., Viovy, N., Zaehle, S., Zeng, N., 2013. Evaluation of terrestrial carbon cycle models for their response to climate variability and to CO2 trends. Glob. Chang. Biol. 19, 2117–2132. https://doi.org/10.1111/gcb.12187.

Piao, S., Wang, X., Park, T., Chen, C., Lian, X.U., He, Y., Myneni, R.B., 2020. Characteristics, drivers and feedbacks of global greening. Nat. Rev. Earth Environ. 1 (1), 14–27.

Pielke Sr., R.A., Wilby, R.L., 2012. Regional climate downscaling: what's the point? EOS Trans. Am. Geophys. Union 93 (5), 52–53.

Platts, P.J., Omeny, P.A., Marchant, R., 2015. AFRICLIM: high-resolution climate projections for ecological applications in Africa. Afr. J. Ecol. 53 (1), 103–108.

Poonia, S., Rao, A.S., 2013. Climate change and its impact on Thar desert ecosystem. J. Agric. Phys. 13 (1), 71–79.

Popp, A., Calvin, K., Fujimori, S., Havlik, P., Humpenöder, F., Stehfest, E., Hasegawa, T., 2017. Land-use futures in the shared socio-economic pathways. Glob. Environ. Chang. 42, 331–345.

Powell, J.M., Pearson, R.A., Hiernaux, P.H., 2004. Crop–livestock interactions in the West African drylands. Agron. J. 96 (2), 469–483.

Prestele, R., Alexander, P., Rounsevell, M.D., Arneth, A., Calvin, K., Doelman, J., Havlik, P., 2016. Hotspots of uncertainty in land-use and land-cover change projections: a global-scale model comparison. Glob. Chang. Biol. 22 (12), 3967–3983.

Rechkemmer, A., 2009. Societal impacts of desertification: migration and environmental refugees?. In: Facing Global Environmental Change. Springer, Berlin, Heidelberg, Germany, pp. 151–158.

Reed, M.S., Fazey, I., Stringer, L.C., Raymond, C.M., Akhtar-Schuster, M., Begni, G., Buckmaster, S., 2013. Knowledge management for land degradation monitoring and assessment: an analysis of contemporary thinking. Land Degrad. Dev. 24 (4), 307–322.

Reich, P.F., Numbem, S.T., Almaraz, R.A., Eswaran, H., 2001. Land resource stresses and desertification in Africa. Agro-Science 2 (2).

Reynolds, J.F., Smith, D.M.S., Lambin, E.F., Turner, B.L., Mortimore, M., Batterbury, S.P., Huber-Sannwald, E., 2007. Global desertification: building a science for dryland development. Science 316 (5826), 847–851.

Riahi, K., Rao, S., Krey, V., Cho, C., Chirkov, V., Fischer, G., Rafaj, P., 2011. RCP 8.5 - a scenario of comparatively high greenhouse gas emissions. Clim. Chang. *109* (1-2), 33.

Riahi, K., Van Vuuren, D.P., Kriegler, E., Edmonds, J., O'neill, B.C., Fujimori, S., Lutz, W., 2017. The shared socioeconomic pathways and their energy, land use, and greenhouse gas emissions implications: an overview. Glob. Environ. Chang. *42*, 153–168.

Roderick, M.L., Greve, P., Farquhar, G.D., 2015. On the assessment of aridity with changes in atmospheric CO2. Water Resour. Res. 51 (7), 5450–5463.

Rogelj, J., Den Elzen, M., Höhne, N., Fransen, T., Fekete, H., Winkler, H., Meinshausen, M., 2016. Paris Agreement climate proposals need a boost to keep warming well below 2 C. Nature 534 (7609), 631–639.

Rohli, R.V., Joyner, T.A., Reynolds, S.J., Ballinger, T.J., 2015. Overlap of global Köppen–Geiger climates, biomes, and soil orders. Phys. Geogr. 36 (2), 158–175.

Rubel, F., Kottek, M., 2010. Observed and projected climate shifts 1901–2100 depicted by world maps of the Köppen-Geiger climate classification. Meteorol. Z. 19 (2), 135–141.

Rubel, F., Brugger, K., Haslinger, K., Auer, I., 2017. The climate of the European Alps: Shift of very high resolution Köppen-Geiger climate zones 1800–2100. Meteorol. Z. 26 (2), 115–125.

Rummukainen, M., 2010. State-of-the-art with regional climate models. Wiley Interdiscip. Rev. Clim. Chang. 1 (1), 82–96.

Ryan, M.G., Archer, S.R., Birdsey, R.A., Dahm, C.N., Heath, L.S., Hicke, J.A., Randerson, J.T., 2008. Land resources: forests and arid lands. In: Janetos, T., Schimel, D. (Eds.), The Effects of Climate Change on Agriculture, Land Resources, Water Resources, and Biodiversity. SAP 4-3. US Climate Change Science Program, Washington, DC, USA, pp. 75–120.

Sachs, J.D., 2007. Poverty and environmental stress fuel Darfur crisis. Nature 449 (7158), 24.

Safriel, U., 2009. Deserts and desertification: challenges but also opportunities. Land Degrad. Dev. 20 (4), 353–366.

Samir, K.C., Lutz, W., 2017. The human core of the shared socioeconomic pathways: Population scenarios by age, sex and level of education for all countries to 2100. Glob. Environ. Chang. 42, 181–192.

Schlesinger, W.H., Reynolds, J.F., Cunningham, G.L., Huenneke, L.F., Jarrell, W.M., Virginia, R.A., Whitford, W.G., 1990. Biological feedbacks in global desertification. Science 247 (4946), 1043–1048.

Schlund, M., Eyring, V., Camps-Valls, G., Friedlingstein, P., Gentine, P., Reichstein, M., 2020. Constraining uncertainty in projected gross primary production with machine learning. J. Geophys. Res. Biogeosci. 125 (11), e2019JG005619.

Schneider, U., Becker, A., Finger, P., Meyer-Christoffer, A., Ziese, M., 2018. GPCC Full Data Monthly Version 2018.0 at 0.5°: Monthly Land-Surface Precipitation from Rain-Gauges Built on GTS-based and Historic Data. *Global Precipitation Climatology Centre (GPCC) at Deutscher Wetterdienst*.

Schwilch, G., Bachmann, F., Liniger, H.P., 2009. Appraising and selecting conservation measures to mitigate desertification and land degradation based on stakeholder participation and global best practices. Land Degrad. Dev. 20 (3), 308–326.

Seager, R., Ting, M., Held, I., Kushnir, Y., Lu, J., Vecchi, G., Li, C., 2007. Model projections of an imminent transition to a more arid climate in southwestern North America. Science 316 (5828), 1181–1184.

Seidl, R., Spies, T.A., Peterson, D.L., Stephens, S.L., Hicke, J.A., 2016. Review: searching for resilience: addressing the impacts of changing disturbance regimes on forest ecosystem services. J. Appl. Ecol. 53, 120–129.

Semenov, M.A., Stratonovitch, P., 2010. Use of multi-model ensembles from global climate models for assessment of climate change impacts. Clim. Res. 41 (1), 1–14.

Sherwood, S., Fu, Q., 2014. A drier future? Science 343 (6172), 737–739.

Sivakumar, M.V.K., 2007. Interactions between climate and desertification. Agric. For. Meteorol. 142 (2–4), 143–155.

Sivakumar, M.V.K., Das, H.P., Brunini, O., 2005. Impacts of present and future climate variability and change on agriculture and forestry in the arid and semi-arid tropics. Clim. Chang. 70 (1–2), 31–72.

Smith, P., Calvin, K., Nkem, J., Campbell, D., Cherubini, F., Grassi, G., Nkonya, E., 2020. Which practices co-deliver food security, climate change mitigation and adaptation, and combat land degradation and desertification? Glob. Chang. Biol. 26 (3), 1532–1575.

Solman, S.A., Blázquez, J., 2019. Multiscale precipitation variability over South America: analysis of the added value of CORDEX RCM simulations. Clim. Dyn. 53 (3), 1547–1565.

Sørland, S.L., Schär, C., Lüthi, D., Kjellström, E., 2018. Bias patterns and climate change signals in GCM-RCM model chains. Environ. Res. Lett. 13 (7), 074017.

Spinoni, J., Vogt, J., Naumann, G., Carrao, H., Barbosa, P., 2015. Towards identifying areas at climatological risk of desertification using the Köppen–Geiger classification and FAO aridity index. Int. J. Climatol. 35 (9), 2210–2222.

Spinoni, J., Barbosa, P., Bucchignani, E., Cassano, J., Cavazos, T., Christensen, J.H., Dosio, A., 2020. Future global meteorological drought hot spots: a study based on CORDEX data. J. Clim. 33 (9), 3635–3661.

Spinoni, J., Barbosa, P., Bucchignani, E., Cassano, J., Cavazos, T., Cescatti, A., Dosio, A., 2021. Global exposure of population and land-use to meteorological droughts under different warming levels and SSPs: a CORDEX-based study. Int. J. Climatol. https://doi.org/10.1002/joc.7302. Accepted.

Stabile, M.C., Guimarães, A.L., Silva, D.S., Ribeiro, V., Macedo, M.N., Coe, M.T., Alencar, A., 2020. Solving Brazil's land use puzzle: Increasing production and slowing Amazon deforestation. Land Use Policy 91, 104362.

Stringer, L.C., Reed, M.S., Dougill, A.J., Seely, M.K., Rokitzki, M., 2007, August. Implementing the UNCCD: participatory challenges. In: Natural Resources Forum, Vol. 31. Blackwell Publishing Ltd, Oxford, UK, pp. 198–211. No. 3.

Sylla, M.B., Elguindi, N., Giorgi, F., Wisser, D., 2016. Projected robust shift of climate zones over West Africa in response to anthropogenic climate change for the late 21st century. Clim. Chang. 134 (1–2), 241–253.

Szelepcsényi, Z., Breuer, H., Sümegi, P., 2014. The climate of Carpathian Region in the 20th century based on the original and modified Holdridge life zone system. Cent. Eur. J. Geosci. 6 (3), 293–307.

Szelepcsényi, Z., Breuer, H., Kis, A., Pongrácz, R., Sümegi, P., 2018. Assessment of projected climate change in the Carpathian Region using the Holdridge life zone system. Theor. Appl. Climatol. 131 (1-2), 593–610.

Tabari, H., Aghajanloo, M.B., 2013. Temporal pattern of aridity index in Iran with considering precipitation and evapotranspiration trends. Int. J. Climatol. 33 (2), 396–409.

Tatli, H., Dalfes, H.N., 2016. Defining Holdridge's life zones over Turkey. Int. J. Climatol. 36 (11), 3864–3872.

Taylor, K.E., Stouffer, R.J., Meehl, G.A., 2012. An overview of CMIP5 and the experiment design. Bull. Am. Meteorol. Soc. 93 (4), 485–498.

Thomas, D.S., 1997. Science and the desertification debate. J. Arid Environ. 37 (4), 599–608.

Thomson, A.M., Calvin, K.V., Smith, S.J., Kyle, G.P., Volke, A., Patel, P., Edmonds, J.A., 2011. RCP4. 5: a pathway for stabilization of radiative forcing by 2100. Clim. Chang. *109* (1-2), 77.

Tschakert, P., 2007. Views from the vulnerable: understanding climatic and other stressors in the Sahel. Glob. Environ. Chang. 17 (3-4), 381–396.

Turner, N.C., 2004. Agronomic options for improving rainfall-use efficiency of crops in dryland farming systems. J. Exp. Bot. 55 (407), 2413–2425.

UN General Assembly, 2015. Transforming our World: The 2030 Agenda for Sustainable Development. Rep- No. A/RES/70/1. Report Available at UN-SDG website. https://sdgs.un.org/publications/transforming-our-world-2030-agenda-sustainable-development-17981. Last accessed on 2 May 2021.

Van Vuuren, D.P., Edmonds, J., Kainuma, M., Riahi, K., Thomson, A., Hibbard, K., Masui, T., 2011. The representative concentration pathways: an overview. Clim. Chang. 109 (1-2), 5.

Van Vuuren, D.P., Riahi, K., Calvin, K., Dellink, R., Emmerling, J., Fujimori, S., O'Neill, B., 2017a. The Shared Socio-economic Pathways: Trajectories for Human Development and Global Environmental Change.

Van Vuuren, D.P., Stehfest, E., Gernaat, D.E., Doelman, J.C., Van den Berg, M., Harmsen, M., Girod, B., 2017b. Energy, land-use and greenhouse gas emissions trajectories under a green growth paradigm. Glob. Environ. Chang. 42, 237–250.
Veron, S.R., Paruelo, J.M., Oesterheld, M., 2006. Assessing desertification. J. Arid Environ. 66 (4), 751–763.
Verstraete, M.M., Scholes, R.J., Smith, M.S., 2009. Climate and desertification: looking at an old problem through new lenses. Front. Ecol. Environ. 7 (8), 421–428.
Vogt, J.V., Safriel, U., Von Maltitz, G., Sokona, Y., Zougmore, R., Bastin, G., Hill, J., 2011. Monitoring and assessment of land degradation and desertification: towards new conceptual and integrated approaches. Land Degrad. Dev. 22 (2), 150–165.
Von Hardenberg, J., Meron, E., Shachak, M., Zarmi, Y., 2001. Diversity of vegetation patterns and desertification. Phys. Rev. Lett. 87 (19), 198101.
Wang, F., Pan, X., Wang, D., Shen, C., Lu, Q., 2013. Combating desertification in China: past, present and future. Land Use Policy 31, 311–313.
Wang, Y., Zhou, B., Qin, D., Wu, J., Gao, R., Song, L., 2017. Changes in mean and extreme temperature and precipitation over the arid region of northwestern China: observation and projection. Adv. Atmos. Sci. 34 (3), 289–305.
Ware, H., 2019. Desertification and population: sub-saharan Africa. In: Desertification. CRC Press, Taylor & Francis, Boca Ratòn, USA, pp. 165–202.
Way, S.A., 2016. Examining the links between poverty and land degradation: from blaming the poor toward recognising the rights of the poor. In: Johnson, P.M., Mayrand, K., Paquin, M. (Eds.), Governing Global Desertification. Routledge, New York, pp. 27–41.
Wu, S., Yin, Y., Zheng, D., Yang, Q., 2005. Aridity/humidity status of land surface in China during the last three decades. Sci. China Series D: Earth Sc. 48 (9), 1510–1518.
Yang, Y., Roderick, M.L., Zhang, S., McVicar, T.R., Donohue, R.J., 2019. Hydrologic implications of vegetation response to elevated CO 2 in climate projections. Nat. Clim. Chang. 9 (1), 44–48.
Yao, J., Liu, H., Huang, J., Gao, Z., Wang, G., Li, D., Chen, X., 2020. Accelerated dryland expansion regulates future variability in dryland gross primary production. Nat. Commun. 11 (1), 1–10.
Yu, Z., Lu, C., Tian, H., Canadell, J.G., 2019. Largely underestimated carbon emission from land use and land cover change in the conterminous United States. Glob. Chang. Biol. 25 (11), 3741–3752.
Zabel, F., Delzeit, R., Schneider, J.M., Seppelt, R., Mauser, W., Václavík, T., 2019. Global impacts of future cropland expansion and intensification on agricultural markets and biodiversity. Nat. Commun. 10 (1), 1–10.
Zarch, M.A.A., Sivakumar, B., Sharma, A., 2015. Assessment of global aridity change. J. Hydrol. 520, 300–313.
Ze-meng, F.A.N., Tian-xiang, Y.U.E., 2005. Temporal and spatial changes pattern of Holdridge life zones and diversity in China. 地理研究 24 (1), 121–129.
Zhang, H.X., Zhang, M.L., Sanderson, S.C., 2013. Retreating or standing: responses of forest species and steppe species to climate change in arid Eastern Central Asia. PLoS One 8 (4).
Zhou, S., Williams, A.P., Lintner, B.R., Berg, A.M., Zhang, Y., Keenan, T.F., Gentine, P., 2021. Soil moisture–atmosphere feedbacks mitigate declining water availability in drylands. Nat. Clim. Chang. 11 (1), 38–44.
Zhu, Z., Piao, S., Myneni, R.B., Huang, M., Zeng, Z., Canadell, J.G., Cao, C., 2016. Greening of the Earth and its drivers. Nat. Clim. Chang. 6 (8), 791–795.